

GEORGE C. MARSHALL SPACE FLIGHT CENTER
HUNTSVILLE, ALABAMA

PROGRESS IN ELECTRIC PROPULSION SYSTEMS

by

Ernst Stuhlinger

FACILITY FORM 502	N 66 81456	_____
	(ACCESSION NUMBER)	(THRU)
	46	None
	(PAGES)	(CODE)
	TMX-57186	_____
	(NASA CR OR TMX OR AD NUMBER)	(CATEGORY)

(Paper to be presented at the International Astronautical Federation XI Meeting in Stockholm, Sweden, 14 - 21 August 1960)

Progress in Electric Propulsion Systems

by
Ernst Stuhlinger¹

ABSTRACT

The transportation capability of propulsion systems with separate power source, expressed by payload ratio, terminal velocity, and acceleration, depends primarily on two basic parameters: the specific power of the system, α , and the total time of propulsion, τ . Highest terminal velocities to be expected with present technologies are 150 to 200 km sec⁻¹; highest accelerations $5 \times 10^{-4} g_0$. The payload ratio depends on the specific mission, it may vary in typical cases between 5 and 95 percent.

Electrothermal or arc-heated systems will operate at exhaust velocities of 10 to 15 km sec⁻¹ ($I_{sp} = 1,000$ to 1,500 sec); they may find application for satellite correction, orbital freight transfer, and lunar freight missions. Electrostatic or ion systems will have exhaust velocities between 40 and 150 km sec⁻¹ ($I_{sp} = 4,000$ to 15,000 sec); they will be useful for lunar freight missions, for unmanned and manned planetary flight, and for deep space probes. Electrodynamic or MFM systems promise to cover a wide range of exhaust velocities from 10 to 1,000 km sec ($I_{sp} = 1,000$ to 100,000 sec). Their technology is not yet developed far enough to encourage the design of an operable propulsion system. Flight tests of the other two systems may begin around 1962 to 1964.

¹Director, Research Projects Division, Marshall Space Flight Center, NASA

Five years ago, a review paper on electric propulsion systems could have mentioned only a handful of studies written by some undaunted optimists in their spare hours [1]. Today, there is hardly one missile and space craft company in the United States that does not have an active group working on electric propulsion systems. The Government supports electric propulsion projects with several million dollars per year, and the National Aeronautics and Space Administration is about to establish a vigorous program for the development of electrically propelled space vehicles. The feasibility, and the usefulness, of electric propulsion systems is a proven fact, at least as far as their theory goes. The remaining problems are concerned with the efficient technical realization of the systems which look simple and straightforward in their principles.

We will divide our review into two parts: at first, we will consider the transportation capabilities of electric propulsion systems, and then we will discuss the present development status of the different kinds of electric space propulsion engines.

Electrical systems, as contrasted to chemical rocket motors, require a separate source of power to eject the propellant. The prime source together with the conversion plant represent a very substantial addition to the dead mass or burnout mass of the rocket vehicle. The reason why electric propulsion systems, at least for some space missions, are superior to chemical rocket engines is because the exhaust velocities of electric systems are many times greater than those which result from the enthalpy release of a fuel-oxidizer reaction in a chemical rocket motor.

The vehicle accelerations developed by electric propulsion systems will always be very small. Electrically propelled vehicles will therefore

be restricted to the space beyond an appreciable atmosphere, and to trajectories where the thrust forces do not have to compete with gravitational forces greater than about $10^{-4} g_0$.

Figure 1 shows very schematically a chemically propelled, and an electrically propelled rocket vehicle. The component M_W includes all the subcomponents required to generate the electric power for the thrust chambers. M_P denotes the propellant mass and M_L represents the payload, and also structural elements as far as they are not parts of the power plant.

The relation between initial mass M_0 , terminal mass M_L , exhaust velocity v , and terminal velocity u for a chemical rocket vehicle that is not subject to drag or gravitational forces is given by Tsiolkovskii's equation

$$\frac{M_L}{M_0} = e^{-\frac{u}{v}} \quad (1)$$

The corresponding equation for electrically propelled vehicles, or more generally for vehicles which require a separate power source reads

$$\frac{M_L + M_W}{M_0} = e^{-\frac{u}{v}}$$

This equation can be developed into a form suitable for the analysis of the vehicle dynamics by introducing the term "specific power" for the ratio of the power contained in the exhaust beam to the mass of the

power-producing plant,

$$\alpha = \frac{W}{M_W}$$

The product of this specific power with the total time of operation, τ , represents the "specific energy" of the system.

$$E^* = \alpha \tau$$

$$\text{Since } W = \frac{\dot{M}}{2} v^2 = \frac{M_P}{2 \tau} v^2 ,$$

we finally obtain [2]

$$\frac{M_L}{M_O} = e^{-\frac{u}{v}} - \frac{v^2}{2 \alpha \tau} \left(1 - e^{-\frac{u}{v}} \right) \quad (2)$$

In a chemical rocket engine, there is no power-producing plant; M_W is zero, and Eq. (2) transforms into Eq. (1).

Figures 2 and 3 represent Eq. (2). The specific energy, $\alpha \tau$, is 10^{13} and 10^{14} erg g⁻¹ in the two diagrams. They show the payload ratio as a function of the exhaust velocity, with the terminal velocity u as a parameter. For any terminal velocity and specific energy, there is one optimum exhaust velocity that leads to a maximum payload ratio. This optimum exhaust velocity depends very little on the terminal velocity;

by inspection, we may deduce a simple rule of thumb from Figs. 2 and 3 [3]

$$v_{\text{opt}} \approx \sqrt{\alpha \tau} \quad (3)$$

For very small payloads, v_{opt} decreases somewhat, and for $M_L \rightarrow 0$ we obtain [4]

$$v_{\text{opt}} = 0.714 \sqrt{\alpha \tau}$$

and

(4)

$$u_{\text{max}} = 1.14 \sqrt{\alpha \tau}$$

For payloads as large as 95 or 98%, we find

$$u_{\text{opt}} \approx 1.4 \sqrt{\alpha \tau}$$

The ratio of optimum exhaust velocity to maximum terminal velocity for $M_L \rightarrow 0$ is a pure number,

$$\left(\frac{v}{u} \right)_{M_L \rightarrow 0} = 0.626$$

which leads to a mass ratio of

$$\frac{M_0}{M_W} = \frac{M_W + M_P}{M_W} = 4.95 \quad (5)$$

This means that an electrically propelled vehicle with vanishingly small payload should carry about 4 times its power plant mass in the form

of propellant in order to reach a maximum terminal velocity, irrespective of any other parameter. Exhaust velocity and terminal velocity will then be given by Eq. (4).

If there is an appreciable payload, the ratio of the terminal velocity to the optimum exhaust velocity, u/v_{opt} , is a function of the payload ratio. This function is plotted in Fig. 4. Very large payload ratios demand a small u/v_{opt} ratio; if the payload is about 14%, the optimum exhaust velocity is equal to the terminal velocity.

The maximum terminal velocity u_{max} which can be reached with optimized exhaust velocity and a given payload ratio depends on the specific energy, $\alpha\tau$. Figure 5 illustrates this relationship.

Of particular interest is the acceleration which can be reached by an electrically propelled space vehicle. The initial acceleration is determined by thrust and initial mass according to

$$a_o = \frac{F}{M_o}$$

or, after substitution of suitable design parameters:

$$a_o = \frac{\sqrt{\frac{2\alpha}{\tau} M_P M_W}}{M_P + M_W + M_L} \quad (6)$$

The acceleration obviously has a maximum for

$$M_P = M_W$$

which leads to

$$a_{o \max} = \sqrt{\frac{\alpha}{2\tau}} \left(1 - \frac{M_L}{M_O} \right) \quad (7)$$

Equation (7) is plotted in Fig. 6 for two different specific power figures, $\alpha = 0.3 \text{ kw kg}^{-1}$ and $\alpha = 10 \text{ kw kg}^{-1}$. If the payload becomes negligibly small, we obtain

$$a_{o \max} = \sqrt{\frac{\alpha}{2\tau}} \quad \text{for } M_L \rightarrow 0.$$

The acceleration of a vehicle optimized for maximum terminal velocity begins with a somewhat smaller initial acceleration, as shown by Eqs. (5) and (6). However, the terminal acceleration is greater than that of a vehicle optimized for maximum initial acceleration. Table I lists accelerations and terminal velocities for the two cases with $M_L = 0$.

The specific power, α , is of decisive influence on the transportation capability of an electrically propelled vehicle. Its magnitude depends on the systems that are available to generate and convert the power, and on the skill of the design engineer. The best choice for a prime power source at present is a fast fission reactor, and a heat cycle with turbo-generator and radiation cooler for conversion. A fission reactor can be built to operate on a constant power level for a few years. Its mass is proportional to its power rather than to its total amount of energy; the performance of the propulsion system is therefore power-limited, as

contrasted to a chemical rocket which is energy-limited. A system of this kind, if built with present-day technologies, would provide a specific power of about 0.1 kw/kg. Figure 7 shows how this figure is anticipated to grow during the next decades. A very promising conversion system is the thermionic converter. Although not yet available in a technical form, it is anticipated that thermionic converters will eventually be superior to rotating systems regarding efficiency and reliability.

The time of propulsion, τ , also plays a dominating role in the theory of propulsion systems with separate power source. It is often difficult to determine the propulsion time for a mission before mass, thrust, and terminal velocity of the vehicle are known. However, reasonable estimates can be made for many lunar and planetary missions even while propulsion parameters are still somewhat uncertain, and more accurate figures can then be developed by iteration.

Our considerations so far were based on propulsion systems with constant thrust and varying acceleration. It can be proven, though, that the transportation capability of vehicles with separate power source improves when the thrust is varied according to a time program [5]. In particular, the payload becomes a maximum at given power, propellant mass, and propulsion system mass, when the thrust is varied in such a way that the acceleration is constant throughout the flight. Figure 8 shows thrust, acceleration, propellant consumption, and exhaust velocity as functions of time for vehicles with constant thrust, and vehicles with constant acceleration. The difference in transportation capability between the two vehicles is shown in Fig. 9 where the payload

ratio M_L/M_0 is plotted versus the terminal velocity u for two different specific energies α . There is indeed a larger payload for the constant acceleration system. It may be questioned though whether this small gain in capability would justify a variable thrust system with its inherent complexity. The relative gain is greatest in vehicles with very small payloads, and with terminal velocities near the theoretical upper limits. However, the additional equipment required to carry out the thrust variation program would more than offset the gain in payload, at least in ion propulsion systems; arc-heated systems will probably be better off in this respect.

Electric propulsion systems will find application in a number of space missions [6]. Near-earth missions, like orbital transfer and lunar flights, will take longer with electric systems than with chemical engines, but the payload capabilities with electric vehicles will be much larger. Flights to Mars and Venus, still with considerably larger payload, will be a little shorter electrically than chemically on a Hohmann transfer ellipse. A deep space probe to the distance of Pluto will be underway three or four years with an electric system, while the Hohmann transfer time would be 45 years. The electric deep space probe would carry about 6 percent payload, while plenty of electric power for instruments and communication would be available from the propulsion system at no extra cost.

Table II lists several space missions with the estimated propulsion times. Applying the formula of Eq. (3), we find the optimum exhaust velocity for each mission, depending only on the specific power α of

the power-producing system. The table lists three values for α , and also the years when these α 's may be available. The exhaust velocities are given in km sec^{-1} , and also as specific impulses I_{sp} .

Our considerations so far are valid for any kind of propulsion system with separate source of power, independent of the propellant material, and of the way in which the propellant particles are accelerated. Several systems are known today, at least theoretically, which fall into this category; they are listed in Table III. Only the electric systems 2, 4, and 5 will be discussed here in more detail.

Electrothermal or arc-heated systems developed from the study of high-intensity electric arcs [7]. An electric discharge burns between a central and a ring-shaped electrode, while the propellant gas is fed into the chamber. Figure 10 shows an arc-heated chamber schematically. Proper cooling of the walls allows average chamber temperatures far above the melting temperatures of the wall materials. The temperature within the arc may be as high as $50,000^\circ\text{K}$; [8] the average temperature of the gas in the chamber is of the order of $3,000^\circ\text{K}$ to $12,000^\circ\text{K}$. A nozzle at the exit of the plenum chamber produces an exhaust velocity given by the equation

$$\sqrt{2 \Delta H} \quad (8)$$

where ΔH denotes that part of the enthalpy of the gas that transforms into kinetic energy of the beam. This equation may be approximated by

$$v = \sqrt{\frac{2 g R T}{W} \left(\frac{k}{k-1} \right) \left[1 - \left(\frac{p_e}{p_c} \right)^{\frac{k-1}{k}} \right]} \quad (9)$$

for ideal gases without dissociation and ionization; R is the gas constant (erg per deg and per mole), and w the molecular weight of the gas. At the temperatures encountered in an arc-heated propulsion chamber, Eq. (8) must be used instead of Eq. (9), and the enthalpies of the propellant gases must be carefully compared at the high chamber temperatures before propellants can be appraised. Hydrogen motors have been operated successfully over extended periods with an exhaust velocity of 10 to 11 km sec ($I_{sp} = 1,000$ to 1,100 sec) at chamber temperatures of about 3,000 °K [9]. At higher temperatures, Li or LiH may be preferable. The merit of a propellant is determined by its available enthalpy at the chamber temperature, by its cooling capabilities, and by its storability. Figure 11 shows the enthalpy of hydrogen versus the temperature at different chamber pressures. It is anticipated that exhaust velocities up to 15 km sec⁻¹ ($I_{sp} = 1,500$ sec) may be obtained within a few years. The limit for arc-heated systems appears to be around 20 to 25 km sec ($I_{sp} = 2,000$ to 2,500 sec) [10]. It is interesting to note that one reason for this limit is the high conductivity of the chamber gas at high temperatures. When this conductivity approaches that of copper, ohmic losses in the external circuit reduce the overall efficiency of the system considerably. At temperatures in the 3,000° to 5,000° range, the efficiency is determined mostly by enthalpy losses, and by nonrecoverable losses to the cooling system. Typical figures of present efficiencies are 50 to 55 percent.

Table II indicates that arc-heated systems will be useful for satellite correction systems, for orbital transfer missions, and for freight transportation to the moon.

One of the advantages of the arc-heated system is the easy controllability of the exhaust velocity. Within fairly wide limits, the power consumption of the engine is independent of the rate of propellant mass flow. Greater mass flow rate means lower average temperature, and therefore lower exhaust velocity, but greater thrust, according to the equation

$$F = \dot{M} v = \frac{2W}{v}$$

It is possible that arc-heated engines will be built for variable propellant flow.

One of the most stringent problems arising with the long-time operation of arc-heated systems is electrode erosion. Promising methods to overcome this danger are under development. Operating times of several hundred hours at exhaust velocities of 10 km sec^{-1} ($I_{sp} = 1,000 \text{ sec}$) and a thrust of one tenth to one half pound per chamber may be available soon.

Electrostatic or ion propulsion systems use electric fields to accelerate charged propellant particles. A schematic diagram of an ion propulsion system is shown in Fig. 12. The expulsion of positive and negative particles at the same rate is necessary in order to keep the vehicle electrically neutral.

The relations between payload ratio, exhaust velocity, terminal velocity, acceleration, specific power, and time of propulsion, as presented above, are independent of the way in which the particles obtain their kinetic energy, and also of the particle mass and charge. However, as soon as the propellant material has been selected, the voltage is

determined which will be required to accelerate the propellant particles to the desired exhaust velocity. Equation (10),

$$v = \sqrt{2 U \frac{\epsilon}{\mu}} \quad (10)$$

which gives the particle velocity as a function of voltage and charge-to-mass ratio, is plotted in Fig. 13. A number of studies concerning these relationships have been published [11].

Table II implies that exhaust velocities between about 10 and 200 km sec⁻¹ ($I_{sp} = 1,000$ to 20,000 sec) will be desirable. The accelerating voltage should not be lower than about 1,500 volts for ion optical reasons, and not higher than about 1000,000 to 2000,000 volts because of the danger of a spontaneous discharge between electrodes. In Fig. 13 this area of preferred operation has been shaded.

The thrust developed by the electrostatic expulsion of particles is given by

$$F = \sqrt{2 W I \frac{\mu}{\epsilon}} = \sqrt{2 \frac{W^2}{U} \frac{\mu}{\epsilon}} \quad (11)$$

where U is the voltage and I the current. If the negative particles are represented by electrons, they will not add appreciably to the thrust because of their small μ/ϵ ratio.

The flow of charged particles through an accelerating field is governed by Child-Langmuir's space charge law [12]

$$i = \frac{\sqrt{2}}{9 \pi} \sqrt{\frac{\epsilon}{\mu}} \frac{U^{3/2}}{d^2} \quad (12)$$

where i = current density

and d = distance between electrodes.

A number of interesting relations derive from Eqs. (11) and (12).

If f denotes the thrust per cm^2 , we find

$$f = \frac{2}{9\pi} S^2 \quad (13)$$

where S = electric field strength

Equation (13) infers that the thrust per cm^2 of an ion engine depends only on the field strength. If S is limited for reasons of electric breakdown to about 10^6 volt cm^{-1} , the highest thrust per cm^2 of an ion engine will be 8 grams.

With

$$I = \dot{M} \frac{\epsilon}{\mu},$$

Equation (12) becomes

$$f = \frac{1}{18\pi} \frac{v^4}{d^2} \left(\frac{\mu}{\epsilon} \right)^2 \quad (14)$$

Considering f a design constant according to Eq. (13), and v a mission constant (Eq. 3), we find that the length of the accelerating gap, d , is proportional to the mass of the particles, μ . The voltage U will also be proportional to the particle mass μ .

Introducing the diameter v of the thrust chamber, we have

$$F = f \pi r^2$$

and obtain

$$F = \frac{1}{18} U^2 \left(\frac{2r}{d} \right)^2 \quad (15)$$

where $\frac{2r}{d}$ is the "aspect ratio" of an ion motor. It is related to the well-known "perveance" of an ion or electron gun, $I/U^{3/2}$, by the equation

$$\frac{I}{U^{3/2}} = \frac{\sqrt{2}}{36} \sqrt{\frac{\epsilon}{\mu}} \left(\frac{2r}{d} \right)^2 \quad (16)$$

"Aspect ratio" and "perveance" of the ion source should be as great as possible for a high thrust. The rather complex interplay of mass-to-charge ratio, perveance, field strength, and thrust in an ion thrust chamber may be understood best by looking at Figs. 14 a and b which show schematic scale drawings of two ion motors of the same area, the same aspect ratio, the same field strength, the same exhaust velocity, the same power, and the same thrust. Accelerating voltages and mass-to-charge ratios are different. The figure illustrates that a motor for larger voltage and larger μ/ϵ - ratio will be lighter, and easier to build. In fact, it will be almost impossible to utilize the permissible maximum field strength of 10^6 volt cm^{-1} in a simple ion motor as shown in Fig. 14 with ions of an atomic weight of the order of 100. With Cesium ions ($A = 133$) and an exhaust velocity of 100 km sec^{-1} ($I_{sp} = 10,000 \text{ sec}$), the distance d would be only 0.07 cm if the full permissible field strength were utilized, resulting in the maximum thrust density of 8 grams per square centimeter. In Fig. 14, a field

strength of 10,000 volts per cm was assumed, leading to a thrust of 0.08 g per cm². These figures are closer to technical realization than the maximum theoretical values.

Fortunately this problem can be greatly relieved by the application of an accelerating-decelerating system in which the charged particles are first accelerated by a relatively high voltage, and then decelerated again to the desired exhaust velocity [13]. Without elaborating further on the theory of the accel-decel system, we consider Fig. 14c where an accel-decel system for the same common parameters as in Fig. 14a and b is drawn to scale; its μ/ϵ -ratio and its exhaust velocity are equal to those of Fig. 14a. Fig. 14c indicates that the accel-decel principle allows to build thrust chambers for atomic particles practically with the same efficiency which is obtainable with simple thrust chambers and heavier particles.

For still heavier particles, like colloid or dust particles, the thrust chamber module would have even larger dimensions, and the accelerating voltage would be higher. Much interest has been concentrated recently on colloidal particles for electrostatic propulsion systems [14]. While thrust chambers for heavy particles would definitely be lighter and simpler than thrust chambers for atomic or molecular ions, there are a number of technical problems which arise with heavy particle propulsion systems; among them are the generation of uniform particles, the propellant feed system, and the uniform charging of the particles to the desired μ/ϵ ratio. While a non-uniformity of the mass and the charge of the particles of several percent would not be critical, the overall performance of the

propellant system would suffer if a sizeable fraction of the particles had a smaller charge, or no charge at all.

The ion source which at present seems to impose the least amount of problems is the cesium-tungsten source. In one form of the source, cesium vapor diffuses through a thin layer of porous tungsten with a pore size of about one micron. When emerging from the pores at the front face, the atoms move along the surface and very soon lose their outermost electrons into the tungsten because the work function of tungsten is greater than the ionization energy of the cesium atoms. The ions leave the surface after a sitting time of microseconds, provided that the surface has a temperature of about 1400 °K. The ionization efficiency of a cesium-tungsten source of this kind is greater than 99%. Other metals than tungsten, like rhenium, are under investigation. It is desirable that the ion source operate at a lower temperature so that heat radiation losses would be reduced. Other types of ion sources, like the duoplasmatron source [15] or the bombardment source [16], show some promising qualities for ion engines. However, before an ion source is appraised for an ion propulsion system, it should be well understood that the current density within the thrust chamber is not primarily governed by the source, but by the accelerating voltage, and by the distance between electrodes. As a rule, a porous plug cesium-tungsten source can easily provide any current density that may be demanded by the thrust chamber. Other properties required from the ion source are:

Small mass per unit emitting area

Uniform velocity of ions at one well defined cross-section

High ionization efficiency

Low power expenditure per ion

Long operating life

Simplicity of design and operation

The most severe technical problem with which the ion engine designer is still confronted is the neutralization of the ion beam immediately behind the thrust chamber. If the space charge represented by the beam were not neutralized, no real beam would develop at all. A cloud of positive ions would form behind the vehicle; image charges on the vehicle would keep the cloud in place, and any further ions emitted in the field of the cloud by the thrust chamber would turn around and fall back on the vehicle. The same would happen to the negative particles, with the result that no net thrust would develop on the vehicle.

The solution to this problem is the mixing of negative and positive particles as soon as the ions have left the thrust chamber. It will not be sufficient to mix the particles in such a way that their currents compensate at any place along the mixed beam,

$$i_+ = n_+ v_+ e_+$$

and

$$i_- = n_- v_- e_-$$

where n is the volume density of the charges, but it will also be necessary that their volume densities be the same,

$$n_- = n_+$$

from a distance on which is roughly equal to the length of the acceleration chamber. Both conditions together make it necessary that the velocities of positive and negative particles in the direction of the beam be the same. If the positive particles are cesium ions, and the

negative particles electrons, this means that the electrons must be accelerated by a potential difference

$$U_e = U_i \frac{\mu_e}{\mu_i} = \frac{1}{250,000} U_i$$

With $U_i = 6800$ volts, U_e would be 2.7×10^{-3} volts, which is less than the average thermal velocity of electrons which are emitted from a hot metal surface. It will not be possible to generate a flow of electrons with such a small uniform velocity. Even the potential field around the ion beam accelerates the electrons in a radial direction to much higher velocities.

This difficulty can be overcome only by injecting the electrons in a direction perpendicular to the beam direction with an initial velocity as low as possible. They will then oscillate laterally through the beam, and drift forward and backward along the beam according to their initial velocity components in the beam direction, and also according to the potential gradients within the beam in beam direction.

The problem of the engine designer is to influence this internal potential gradient by external electrodes in such a way that no electrons drift backwards, and that those which drift forward do so with the velocity of the positive particles. Very fortunately, there seems to occur a kind of a self-regulating effect between positive beam and negative electrons which allows just the right number of electrons to spill out of the original reservoir and to drift with the ions. It should be noted, though, that after beam neutrality has been achieved at one place near the injection point, it will be maintained further downstream only

when the longitudinal electric field is zero everywhere. Local fluctuations of field strength and beam neutrality are allowed, but they must not extend over distances larger than about the length of the acceleration chamber. Figure 15 illustrates schematically a thrust chamber with beam neutralization.

Neutralization would be easier to achieve if the electron emitters were placed inside the beam itself. This arrangement could lead to serious corrosion and ablation of the emitting surfaces; however, the emitters might be built in such a way that they are replaced by new ones either periodically or in a continuous fashion. The electrons would then only have thermal energies of the order of one ϵV within the beam. If used in conjunction with an acceleration-deceleration system, the electrons would find an uphill potential field towards the exit orifice of the decel state, and would therefore turn around before impinging on the exit electrode. The simplified, one-dimensional theory (16a) infers that a steady state will be reached in which electrons from the emitters fill the beam to neutrality. The beam potential fluctuates with small amplitude around a constant value. If electron emitters and decelerating electrode are joined together to form a "neutralizing grid", the spacing between accelerating electrode and neutralizing grid has no influence on the thrust and exhaust velocity of the beam, because electrons will drift backward and fill the space to a point close to the accel electrode, regardless of how far downstream the neutralizing grid is placed. Further experiments will have to verify the feasibility of this system.

Very valuable contributions to the problem of beam neutralization have been made with analog simulators of particle trajectories [17] . The potential fields are simulated in an electrolytic tank, with small auxiliary electrodes representing space charges. Direction and strength of the electric field is measured with a little probe, and the trajectory of a particle is computed as a result of the force field measured throughout the tank.

The problem of matching the velocities of positive and negative particles for beam neutralization would be much easier if the masses of both kinds of particles were about equal. Studies are underway at several places to develop sources for negative ions which are as simple and as efficient as the cesium-tungsten source. If these attempts should prove successful, an ion engine including ion source, thrust chamber, and beam neutralization would be as simple as shown in Fig. 16.

Several contracts for the development of laboratory models of small ion engines are presently underway in the United States. The models will produce a thrust of the order of 1/100 to 1/10 pound at an exhaust velocity of the order of 50 km sec^{-1} ($I_{sp} = 5,000 \text{ sec}$) probably during 1961. It should be mentioned, though, that laboratory models can be successfully operated even before the problem of beam neutralization has been completely solved, because chamber walls, residual gases, and other influences which cannot be avoided in a vacuum tank, help to form and sustain an ion beam of considerable length. The real test of an ion engine must take place onboard a high altitude probe or satellite under perfect space conditions. It is hoped that space tests of ion engine prototypes can be initiated in 1962. Even short time tests of several

minutes duration, powered by batteries, can fully prove the correct operation of beam formation and beam neutralization under space conditions. Testing of the engine for long-time capabilities should then be taken up as a next phase in the development program.

Once the ion engine is developed, it will find application for freight flights to the moon, for unmanned and manned planetary missions, and for instrumented probes to the outer fringes of our planetary system.

Electrodynamic or magnetofluidmechanic systems, like arc heated systems, do not suffer from the problem of space charge neutralization. The driving force is provided by a varying magnetic field, or by combined electric and magnetic fields. The propellant is ionized to a high degree, but the charges are not separated; they form a neutral plasma. If an electric field is applied to a plasma, particles of opposite signs move in opposite directions; if a magnetic field is present with its direction perpendicular to that of the electric field and to the velocity vector of the particles, a motion results as indicated in Fig. 17. Diagram a shows the motion of two particles in a strong electric field, diagram b in a weaker field. The force p acting on each particle is given by

$$p = \frac{e}{c} \vec{v} \times \vec{H}$$

or, if the current density i is introduced:

$$p_i = \frac{1}{c} \vec{i} \times \vec{H}$$

The drift velocity ϕ shown in Fig. 17b is a function of the two fields only:

$$\phi = c \cdot \frac{\vec{E} \times \vec{H}}{H^2}$$

The laws of plasma motion under the combined forces of electric and magnetic fields are obtained by simultaneous application of the equations of fluid flow and of the electrodynamic theory. Rather than trying to solve an array of these equations for a simplified experimental arrangement, we will analyze qualitatively a plasma engine which has been operated, and which shows many of the characteristic features of MFM Systems [18]. Figure 18 shows a cross section through the device. It consists of two concentric cylinders, with an insulating plug at one end. Hydrogen under low pressure enters at H; a high frequency discharge is maintained between d and d'. A propulsive pulse is initiated by closing the switch S, thereby discharging the condenser bank C through the gas. The flow of current through the gas is indicated in the drawing. It generates a toroidal magnetic field, which, together with the radial electric field, exerts a force upon the radial current in the axial direction. Under actual working conditions, the radial velocity of the charged particles under the force of the voltage difference is of the order of 10^9 cm sec⁻¹; the axial velocity may reach 4×10^7 cm sec⁻¹. The moving plasma drives the unionized gas between the cylinders along in the form of a shock wave. A permanent, relatively weak magnetic field in axial direction, generated by the two coils indicated in the sketch, forms a "magnetic bottle" which keeps the

hot plasma away from the walls. - The efficiency of this system, expressed as the ratio of electric energy input to kinetic beam energy, is of the order of 30%. Much simpler, but also less efficient MFM propulsion systems are obtained if an arc is struck between two parallel wires or two parallel plates (Fig. 19a), [19] or between a short central and a ring-shaped electrode (Fig. 19b) [20]. In either case, the arc moves out under the force of its own magnetic field. In the backstrap propulsor [21], one of the two conductors is placed along the rear side of the discharge chamber in such a way that the magnetic field produced by the discharge current helps to push the plasma out. Figure 19c shows this arrangement.

As contrasted to ion propulsion systems, MFM systems have the advantage of relatively high densities of the plasma flow, and of easy controllability of the exhaust velocity between wide limits. Their disadvantages are the large masses of auxiliary equipment, like condensers and magnetic field coils, and their low efficiencies which only rarely reach 30 to 40%. The greater part of the electromagnetic energy is transformed into heat. An extremely short discharge time of the condenser is essential in order to keep the penetration depth of the induced currents into the plasma small, and to reduce the dissipation of electromagnetic energy. In the travelling wave propulsor [18], a tube containing the propellant is surrounded by a distributed L - C circuit. If a condenser is discharged across the input terminals, a magnetic wave travels through the tube with the velocity

$$v = \frac{1}{\sqrt{LC}}$$

where

L = inductivity

C = capacity of one segment of circuit

It ionizes the gas and drives the plasma ahead like a plug (Fig. 19d).

Interest in magnetofluidmechanic devices has arisen recently from five different sources: they offer a convenient method to study plasma physics in general; they provide a technique to generate shockwaves of extremely high Mach numbers for the study of re-entry phenomena; they may help to eventually achieve a controlled fusion reaction; they facilitate the understanding of processes in hot star atmospheres; and, finally, they may provide a propulsion device for certain space missions. At the present state of development, the efficiencies are still too low, the masses too large, and the lifetimes too short to make an MFM propulsor an attractive propulsion system. This situation may well change with further technical development.

Electric propulsion devices have been studied to an extent where the feasibility and usefulness of at least two systems appears very likely: arc-heated systems, and ion systems. The first flight tests on satellites may begin in 1962, while space missions may be flown with arc-heated systems from about 1963 on, and with ion systems from 1964 or 1965 on. Electric systems will be competitive with chemical systems on heavy freight missions in near-earth space; on unmanned and manned missions to Venus and Mars; and very particularly on missions to more distant planets, and into deep space.

TABLE I

Parameter to be maximized	Exhaust velocity v	Terminal velocity u	Initial acceleration a	Terminal acceleration a_t
u	$0.714\sqrt{a\tau}$	$1.14\sqrt{a\tau}$	$0.565\sqrt{a/\tau}$	$2.82\sqrt{a/\tau}$
a_0	$1.41\sqrt{a\tau}$	$0.981\sqrt{a\tau}$	$0.707\sqrt{a/\tau}$	$1.41\sqrt{a/\tau}$
Ratio	0.506	1.16	0.80	2.0

Exhaust velocity, terminal velocity, and accelerations of vehicles with maximized terminal velocity, and with maximized initial acceleration. Total initial mass, travel time, and specific power are the same for both vehicles. The payload is negligibly small in both cases.

TABLE II

Optimum Exhaust Velocities for Various Space Missions at
Three Different Specific Power Figures

Mission	Propulsion Time		Exhaust Velocity Km sec ⁻¹		
			$\alpha = 0.1$ Kw Kg ⁻¹ 1965	$\alpha = 0.3$ Kw Kg ⁻¹ 1970	$\alpha = 10$ Kw Kg ⁻¹ 1980
Satellite Correction	10 days	8.6 x 10 ⁶	9.3	16	93
Orbital Transfer	20 days	1.8 x 10 ⁶	13.5	23.4	135
Lunar Ferry	60 days	5.2 x 10 ⁶	23	40	230
Mars-one way	200 days	1.8 x 10 ⁷	42.5	74	425
Mars-return	450 days	3.9 x 10 ⁷	62	108	620
Jupiter, Saturn	2 years	6.3 x 10 ⁷	80	142	800
Deep Space	3 years	9.5 x 10 ⁷	97	168	970

TABLE III

Propulsion Systems With Separate Power Source

1. Nuclear heated
2. Electrothermal (arc-heated)
3. Solar heated
4. Electrostatic (ion)
5. Electrodynamic (MFM)
6. Solar sail
7. Partial photon
8. Ideal photon

REFERENCES

1. Goddard, R. H. (1959). R. H. Goddard, An Autobiography-Robert H. Goddard Notebook dated Sep 6, 1906. Astronautics 4, 4, 24.
 Oberth, H. (1929). "Wege zur Raumschiffahrt." R. Oldenbourg, München-Berlin.
 Ackeret, J. (1946). Helvet. Physica Acta 19, 103.
 Seifert, H. S., Mills, M.W., & Summerfield, M. (1947). "Physics of Rockets." Amer. Journ. of Phys. 15, 255.
 Shepherd, L.R. & Cleaver, A.V. (1948-1949). J. Brit. Interplan. Soc. 7, 185, 234; J.B.I.S. 8, 23, 59.
 Forbes, G.F. (1950). "The Trajectory of a Powered Rocket in Space." J. Brit. Interplan. Soc. 9, 75.
 Lawden, D. F. (1950). "Note on a Paper by G. F. Forbes." J. Brit. Interplan. Soc. 9, 230.
 Spitzer, Jr., L. (1952). "Interplanetary Travel Between Satellite Orbits." Amer. Rocket Soc. Journ. 22, 92.
 Preston-Thomas, H. (1952). J. Brit. Interplan. Soc. 11, 173.
 Stuhlinger, E. (1954). "Possibilities of Electrical Space Ship Propulsion." V. Internat'l Astron. Cong., Innsbruck, p. 100.
 Stuhlinger, E. (1955). "Electrical Propulsion Systems for Space Ships with Nuclear Power Source." J. Astronautics, Vol 2, p. 149; Vol 3, p. 11, 33.
2. Langmuir, D.B. (1956). "Optimization of Rockets in Which Fuel is Not Used as Propellant." Ramo-Wooldridge Corp. Rpt. ERL 101, (Sep).
 Stuhlinger, E. (1957). "Design and Performance Data of Space Ships With Ionic Propulsion Systems," VIII. Internat'l Astron. Congress,

Barcelona, 1957. Proceedings by Springer Verlag, Vienna, pg. 403, 1957.

"Advanced Propulsion Systems for Space Vehicles," IX. Internat'l Astronautical Congress, Amsterdam, 1958. Proceedings by Springer Verlag, Vienna, pg. 232, 1958.

Irving, J.H. (1956). "Optimum Program for Single Stage Rockets in Which Expellant is not the Source of Power." Ramo-Wooldridge Corp. rpt.

Irving, J.H. (1958). Space Technology Course, UCLA.

3. Stuhlinger, E. (1960). "Handbook of Astronautical Engineering," Ed. H. H. Koelle, McGraw Hill, in print. (1960).

4. Langmuir, D.B., "Low Thrust Flight: Constant Exhaust Velocity in Field-free Space." Space Technology, ed by H. Seifert, John Wiley & Sons, 9-01, 1959.

Kaufmann, H.R., "One-Dimensional Analysis of Ion Rockets." NASA Rpt TN D-261.

Stuhlinger, E. & Seitz, R.N. (1960). "Electrostatic Propulsion Systems for Space Vehicles," chapter to be included in the 1960 Edition of "Advances in Space Science," edited by F. I. Ordway, III, Academic Press, New York.

5. Irving, J.H. (1959). "Low-thrust flight: Variable Exhaust Velocity in Gravitational Fields," in Space Technology, Ed. by H. S. Seifert, John Wiley and Sons, New York, pg. 10-01, 1959.
6. Stuhlinger, E. (1957) "Flight Path of an Electrically Propelled Space Ship," Jet Propulsion, Vol. 27, No. 4, pg. 410, 1957.

- Ehricke, K.A., "Interplanetary Operations," Space Technology, John Wiley & Sons, New York, pg. 8-01, 1959.
- Moeckel, W.E. (1959). "Propulsion Methods in Astronautics," Lewis Flight Propulsion Laboratory, NASA, 1959.
- Evaard, J.C. (1959). "Electric Space Propulsion," Lewis Research Center, NASA, 1959.
- Stuhlinger, E. (1960). "Flight Missions for Electrically Propelled Space Vehicles," American Astronautical Society, New York, 1960.
7. Finkelburg, W., "The High Current Carbon Arc and its Mechanism." J. Appl. Phys. 20, 1949.
 8. Cann, Gordon, Adriano Ducati, and Vernon Blackmon, "Experimental Studies on the Thrust from a Continuous Plasma Jet," Paper presented at Advanced Propulsion Systems Symposium, Rocketdyne, AFOSR, Los Angeles, California, 1957.
 9. Giannini, G.M., "The Plasma Jet," Scient. American, Vol. 196, p. 80 1957.
 10. Heller, G. (1959). "The Plasma Jet as an Electric Propulsion System for Space Application," ARS 1040-59, November 1959.
 11. Boden, R.H. (1957). "The Ion Rocket Engine." Rocketdyne Rpt. R-645P.
Baldwin, G.C., Downing, R., Edgar, R.F., Goodale, E.E., Sawyer, J.F., & Stauffer, L.H. (1958). "Experimental Investigation Pertinent to an Ionic Propulsion Concept," G.E. General Engr. Lab. Rpt. No., 58GL355.

Eilenberg, S.L. & Huebner, A.L.C. (1959). "Engineering & Scientific Problems of Ion Propulsion," ARS Meeting, San Diego, California.

Langmuir, D.B. "Problems of Thrust Production by Electrostatic Fields." Vistas in Astronautics, Vol. II. Pergamon Press, 191, 1959.

Forrester, A.T. & Speiser, R.C. (1959). "Cesium Ion Propulsion," Astronautics, Vol. 4, No. 10, 34.

Fox, R.H., "Study of Electric Propulsion Systems for Space Travel." UCRL 5478, Lawrence Radiation Laboratory, Feb 6, 1959.

Krulikowski, B.K., "An Alkali Metal Ion Source." IPU 59-08, Naukovi Povidomlemia Fizyka, Kiev U. No. 1, 1956, pp. 11 - 12.

Stavisskii, Y.Y., Bondarenko, I.I., Krotov, V.I., Lebedev, S.Y., Pupko, V.Y., and Stumbur, E.A., "Experiment to Obtain Reaction Thrust in a Laboratory Model of an Ion Engine." Soviet Physics & Tech. V. 4, #8.

Childs, J.H., "Design of Ion Rockets and Test Facilities." IAS Nat'l Summer Meeting, Los Angeles, Calif., June 1959.

Stuhlinger, E., & Seitz, R.N. (1959). "Some Problems in Ionic Propulsion Systems." I.R.E. Trans. Military Electronics MIL-3,27.

Boden, R.H., "Electrical Space Propulsion," Rocketdyne Rpt, 1959.

Childs, J.H. (1959). "Design of Ion Rockets and Test Facilities." Paper No. 59-103, Inst. Aero. Sci., 1959.

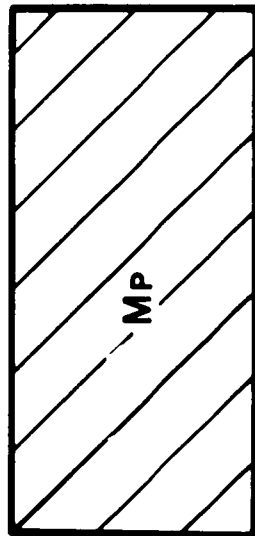
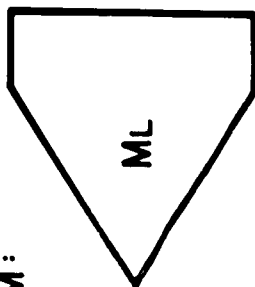
Edwards, R.N. & Kuskevics, G., "Cesium Ion Rocket Research Studies," Paper No. 59-AV-32, ASME, 1959.

12. Child, E.D. (1911). "Discharge from Hot CaO." Phys. Rev. 32, 492.
Langmuir, I. (1913). The Effect of Space Charge and Residual Gases on Thermionic Current in High Vacuum." Phys. Rev. 2, 450.
13. Raether, M.J. and Seitz, R.N., ARS. paper 884-59, 1959,
14. Schultz, R.D., "Some Technical Problems Associated with a Charged-Colloid Propulsion System," Aerojet General Corp. Rpt TM No. 808, 1958.
Wiech, R.E., "Heavy Particle Propulsion Research," Thiokol Chemical Corp. Rpt RMD-1155-52, 1959.
Rocketdyne Rpt R-2066P, "Proposed Propellants for Electrical Propulsion Systems," 1959.
15. Von Ardenne, M., "New Developments in Applied Ion and Nuclear Physics," Lib. Trans. 758, AERE, Harwell (Berkshire, 1957).
Also: Private Communication, Dr. J. Gale, Goodrich-High Voltage Engineering Corp., March 1960.
16. Meyerand, R.G. & Brown, S.C., "High Current Ion Source," Review of Scientific Instruments 30, 110, 1959.
17. Duzer, T. Van, & Brewer, G.R., "Space Charge Simulation in an Electrolytic Tank," J. Appl. Phys., March 59.
18. Patrick, R.M., "A Description of a Propulsion Device Which Employs a Magnetic Field as the Driving Force," Second Annual AFOSR Astron. Symp., Denver, Col. (1958).
Patrick, R.M., "High Speed Shock Waves in a Magnetic Annular Shock Tube," AFOSR-TN-59-845, Second Symposium on Advanced Propulsion Concepts, Boston, Mass., 7-8 Oct., 1959.

- Kantrowitz, A.R. & Petchek, H.E., "Magnetohydrodynamics," Edited by R.K.M. Landshoff, Stanford Univ. Press, p. 3 (1957).
19. Resler, E.L., Jr., & Sears, W.R., "The Prospects for Magneto-aerodynamics," Journ. Aero/Space Sciences, Vol. 24, No. 4, 1958.
- Clauser, M.U., "Magnetohydrodynamics," Chapter 18 of "Space Technology," Ed. by H. Seifert, John Wiley & Sons, 1959.
- Sears, W.R., "Magnetohydrodynamic Effects in Aerodynamic Flows," ARS Journal, Vol. 29, p. 397, 1959.
- Ghai, M. L., "Plasma Propulsion for Space Applications," ARDC-OSR Contractor's Conference on Ion and Plasma Research, Oct. 1, 1958.
20. Bostick, W., "Experimental Studies of Plasmoids." Phys. Rev. 106 April-June, 1957.
21. Kolb, A.C., "Production of High-Energy Plasmas by Magnetically Driven Shock Waves." Phys. Rev. 107, 345, 1957.
- 16a. Mirels, H., & Rosenbaum, B.M.: "Analysis of One-Dimensional Ion Ion Rocket with Grid Neutralization," NASA-TN-D-266, 1960.
- Kaufman, H.R.: "One-Dimensional Ion Rockets," NASA-TN-D-261, 1960.

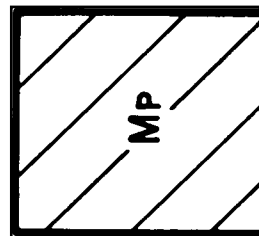
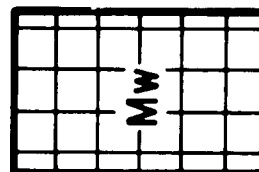
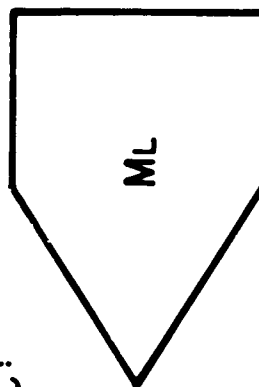
Figure	INDEX OF ILLUSTRATIONS	Page
1a	Comparison Between Chemically & Electrically Propelled Vehicles	36
1b	Components of Space Vehicle With Separate Power Source	37
2	Payload Ratio as a Function of Exhaust Velocity and Terminal Velocity ($\alpha\tau = 10^{13}$)	38
3	Payload Ratio as a Function of Exhaust Velocity and Terminal Velocity ($\alpha\tau = 10^{14}$)	39
4	Ratio of Terminal Velocity to Optimum Exhaust as a Function of payload ratio	40
5	Payload Ratio as a Function of the Maximum Terminal Velocity	41
6	Initial Acceleration of Vehicle as a Function of Payload and Specific Power	42
7	Expected Growth of Specific Power of Electric Power Supplies	43
8	Comparison of Propulsion Systems With Constant Thrust (---) and Constant Acceleration (—)	44
9	Comparison of Propulsion Systems With Constant Acceleration and Constant Thrust	45
10	Arc-heated Propulsion Engine	46
11	Enthalpy of Hydrogen as a Function of Temperature and Chamber Pressure	47
12	Schematic of Ion Propulsion System	48
13	Exhaust Velocity as a Function of Particle Mass and Accelerating Voltage (Each particle is assumed to carry one unit charge.)	49
14	Ion Thrust Chambers of Equal Performance (Schematic)	50
15	Ion Beam With Electron Injection (Schematic)	51
16	Arrangement of Negative and Positive Ion Sources With Acceleration Chambers (Schematic)	52
17	Motions of Charged Particles in Electric and Magnetic Fields	53
18	Cross Section Through Magnetofluidmechanic Propulsion Engine (Schematic)	54
19	Various Types of Electrodynamic Propulsion Systems	55

CHEM:



$$\frac{M\tau}{M_0} = \frac{M_L}{M_0} = \frac{u}{-v} e$$

ELEC:



$$\frac{M\tau}{M_0} = \frac{M_L + M_W}{M_0} = \frac{u}{-v} e$$

$$\frac{W}{M_W} = \alpha ; \quad \frac{M_L}{M_0} = \frac{u}{-v} e - \frac{v^2}{2\alpha c^2} \left(1 - \frac{u}{-v} e \right)$$

FIG. 1a - Comparison Between Chemically and Electrically Propelled Vehicles

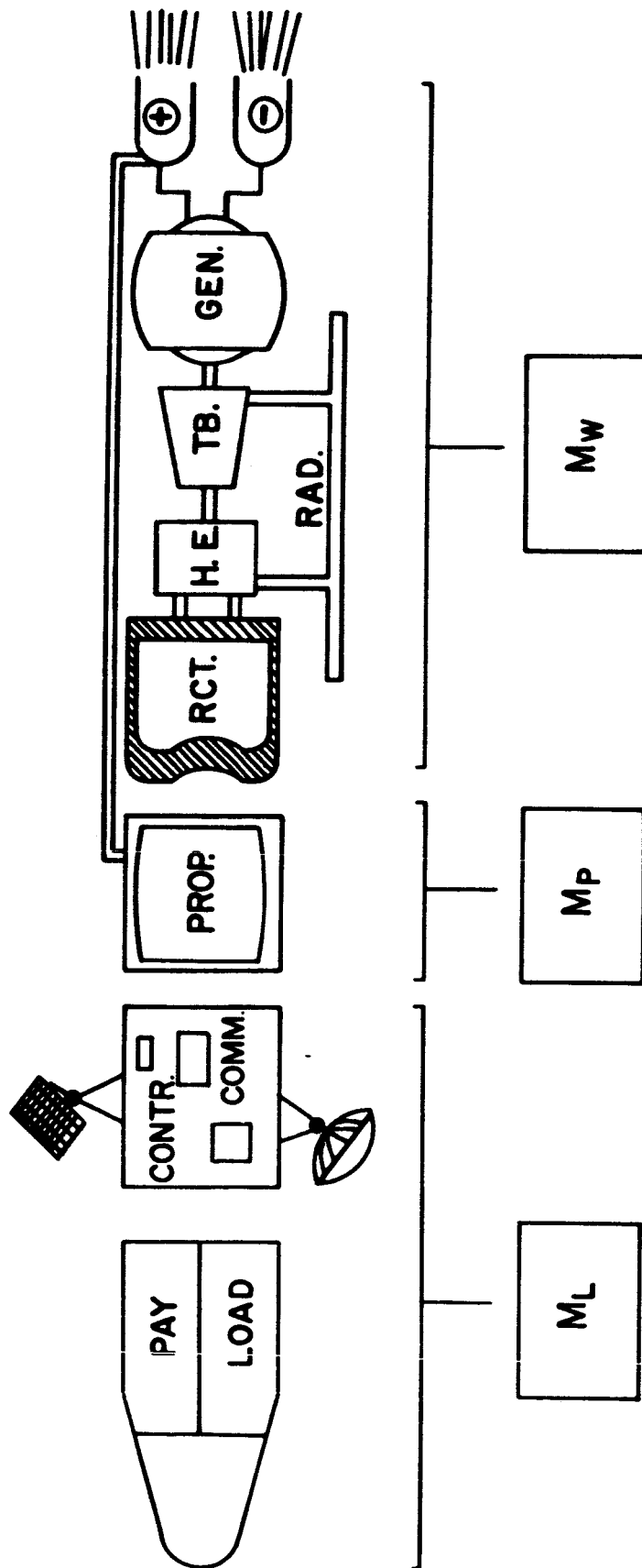


FIG. 1b - Components of Space Vehicle With Separate Power Source

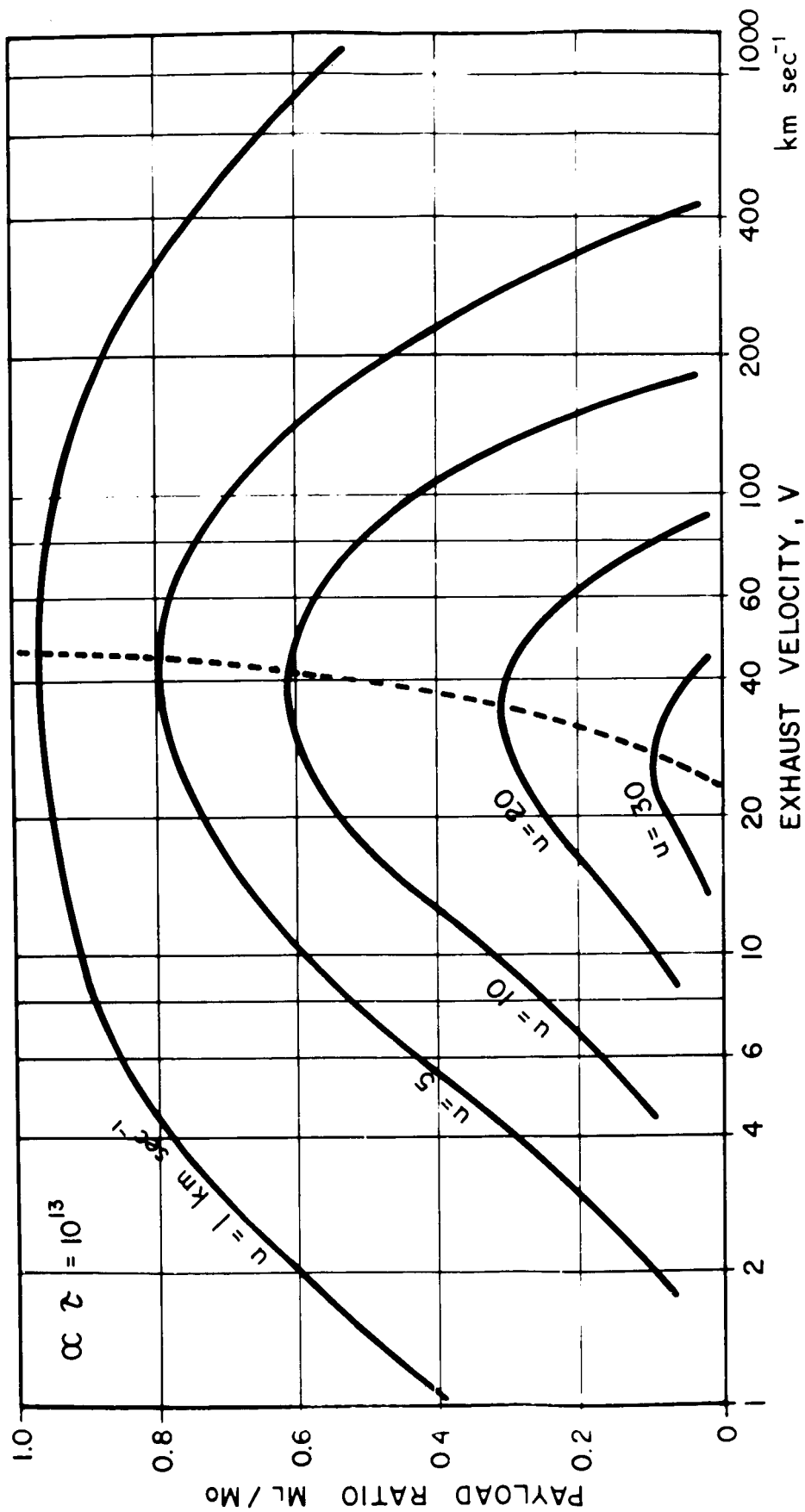


FIG. 2 - Payload Ratio as a Function of Exhaust Velocity and Terminal Velocity ($\alpha \tau = 10^{13}$)

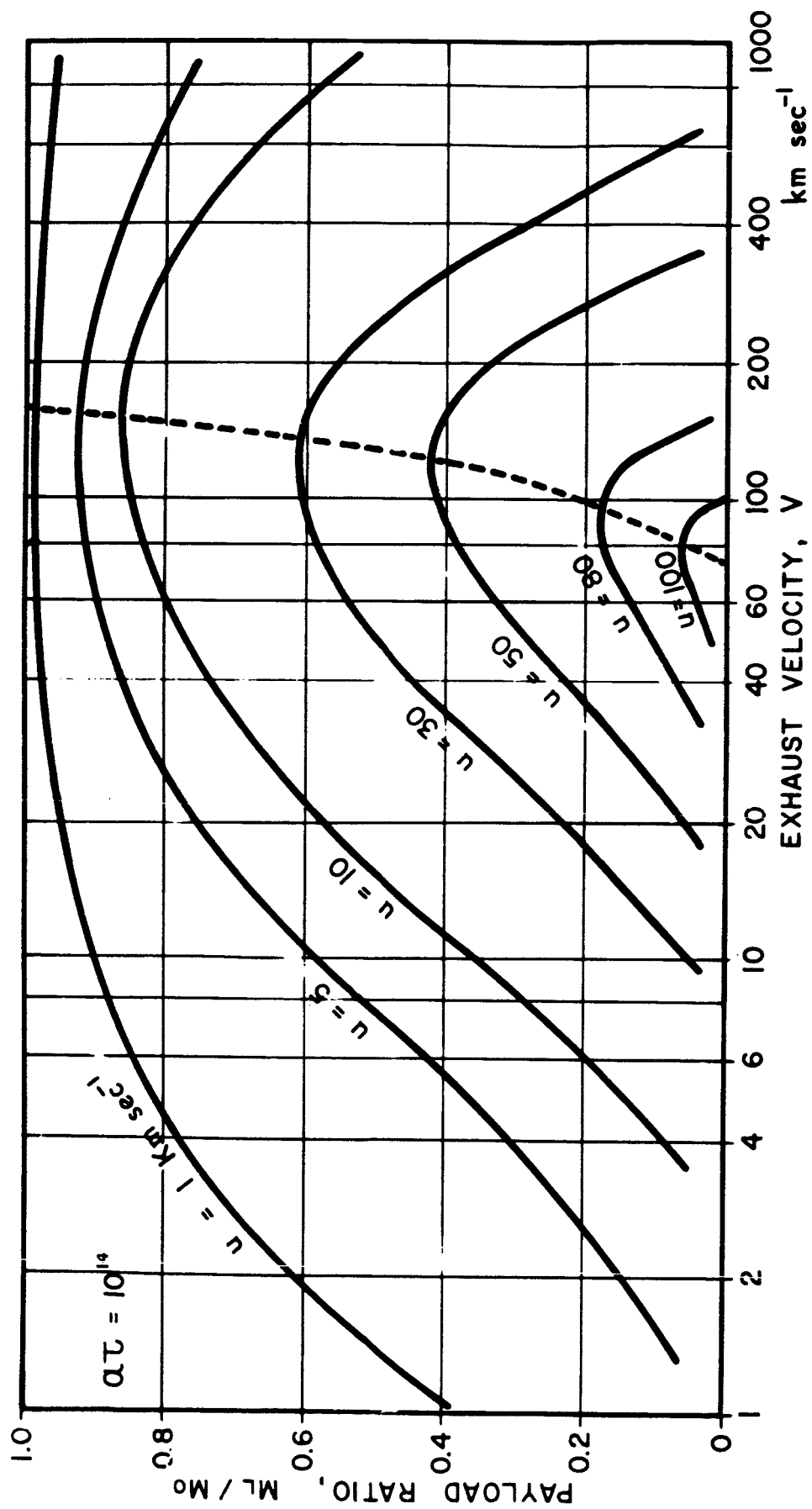


FIG. 3 - Payload Ratio as a Function of Exhaust Velocity and Terminal Velocity ($\alpha\tau = 10^{14}$)

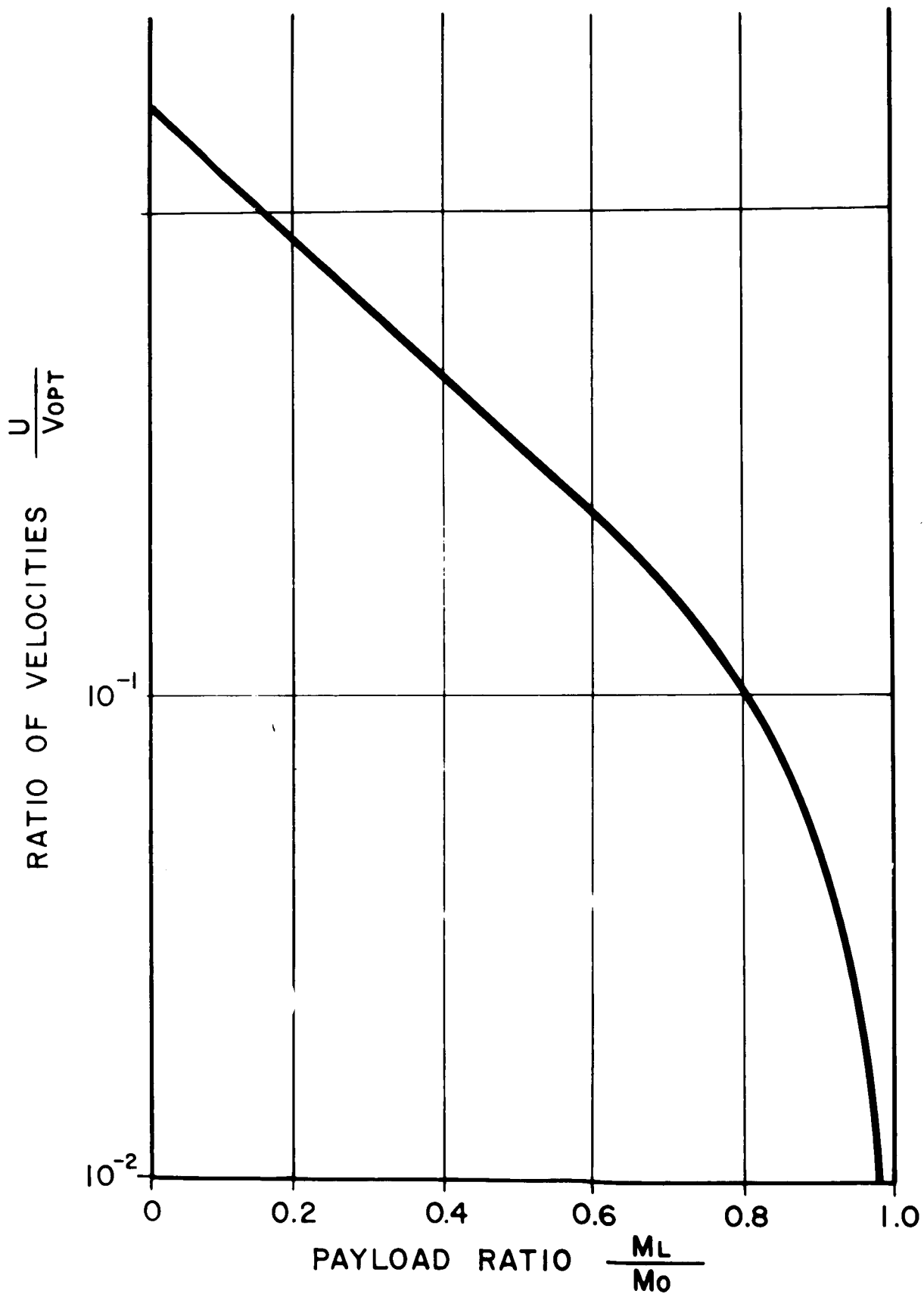


FIG. 4 - Ratio of Terminal Velocity to Optimum Exhaust Velocity as a Function of Payload Ratio

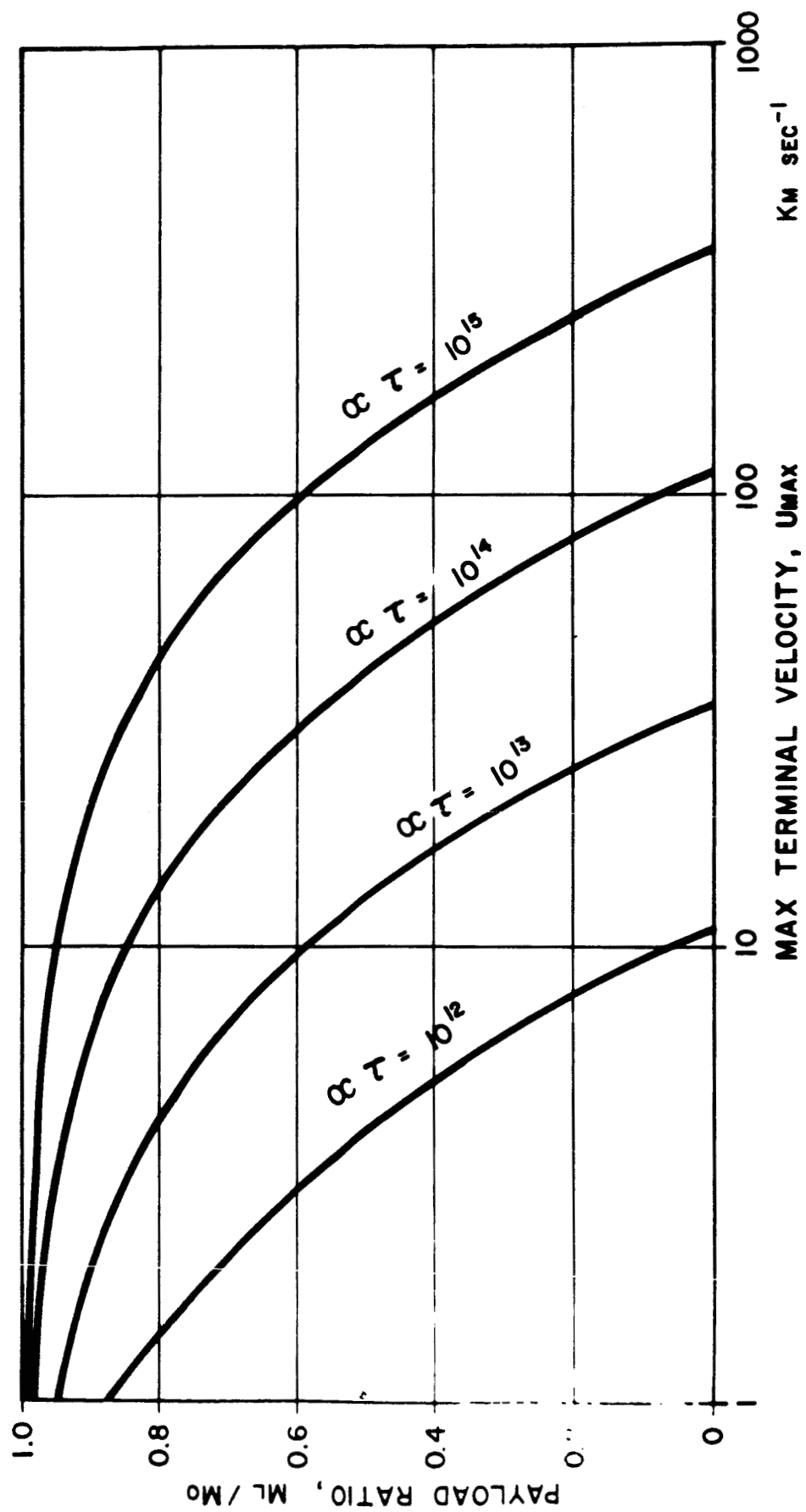


FIG. 5 - Payload Ratio as a Function of the Maximum Terminal Velocity

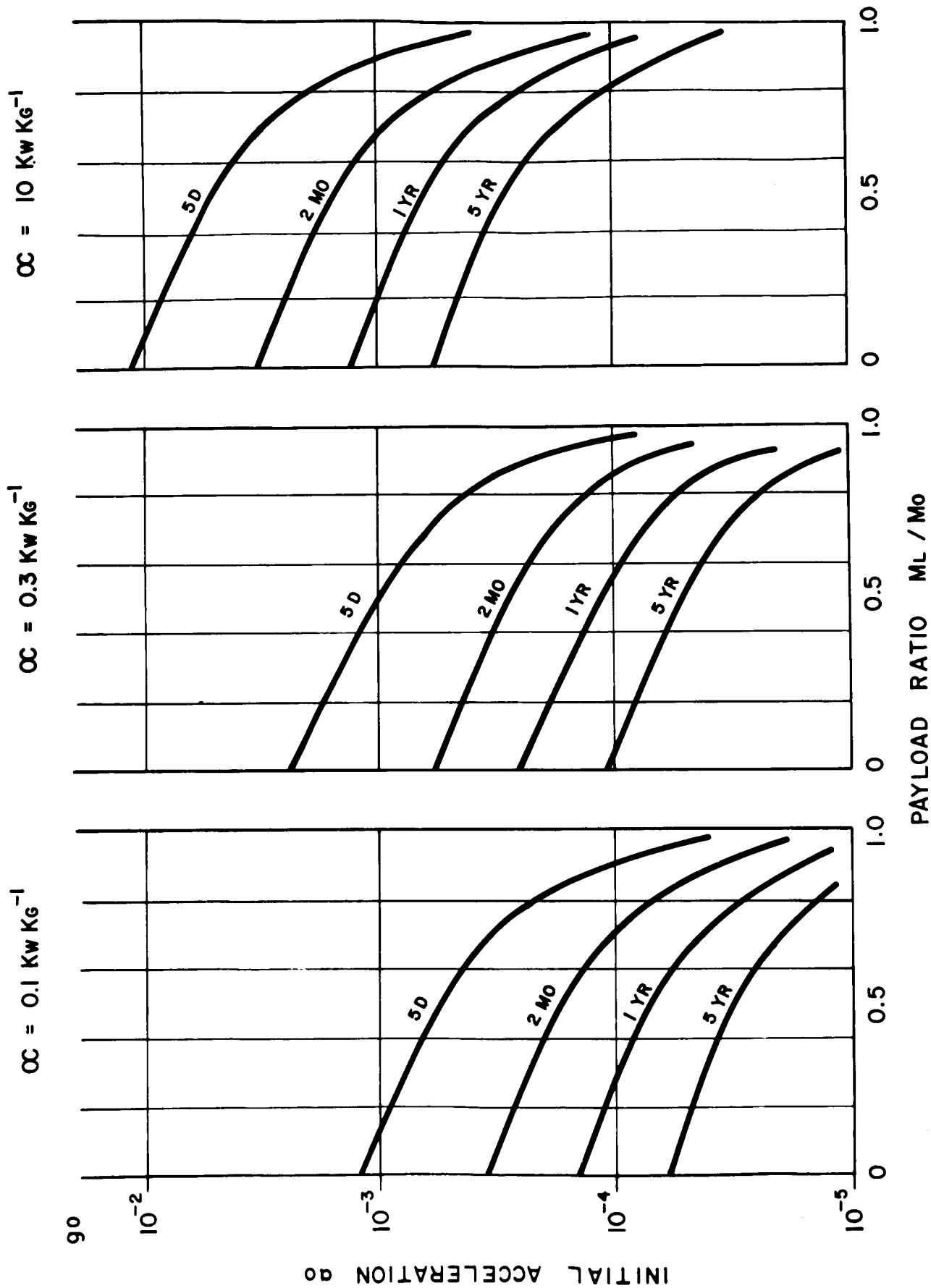


FIG. 6 - Initial Acceleration of Vehicle as a Function of Payload and Specific Power

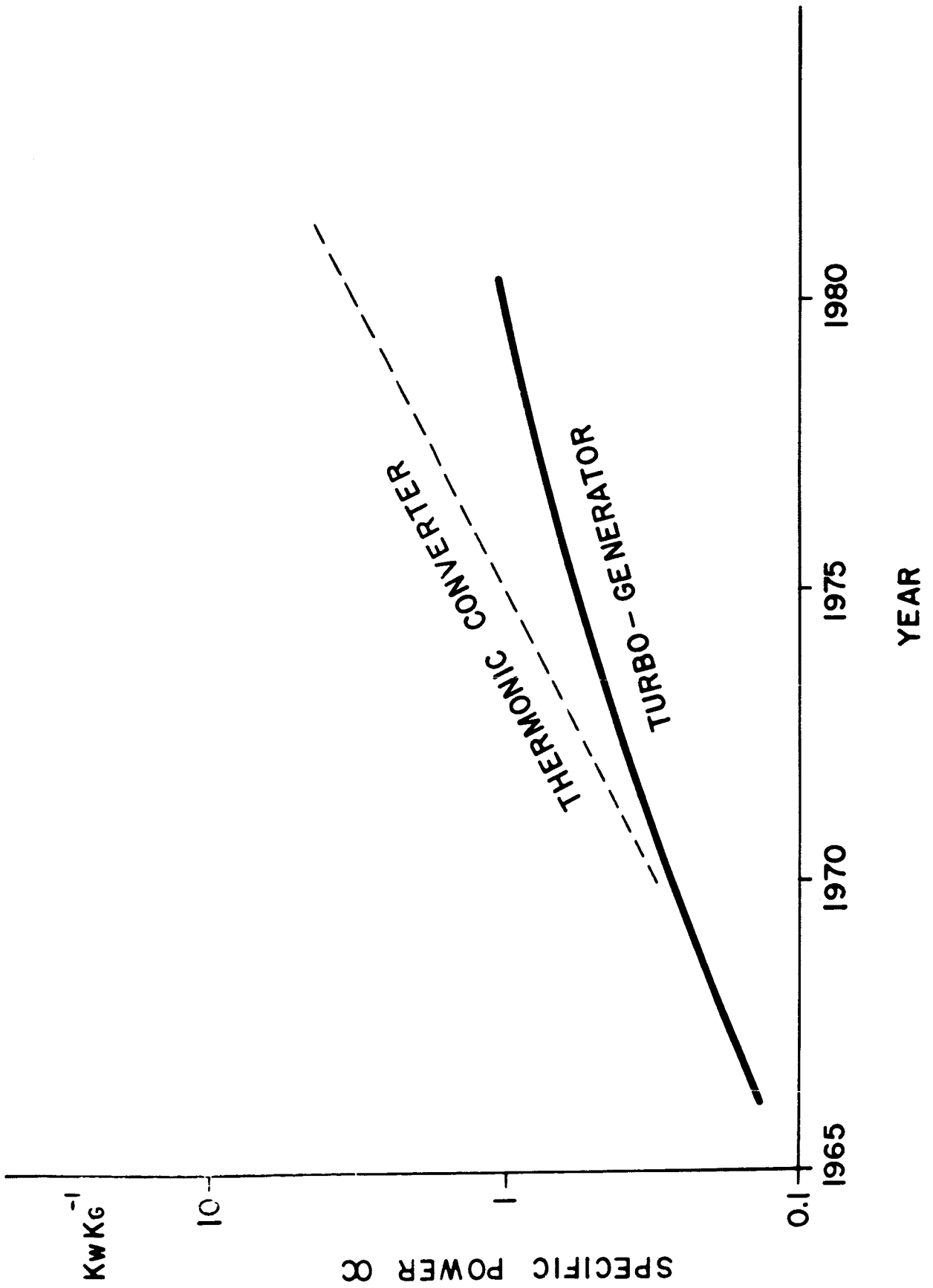


FIG. 7 - Expected Growth of Specific Power of Electric Power Supplies

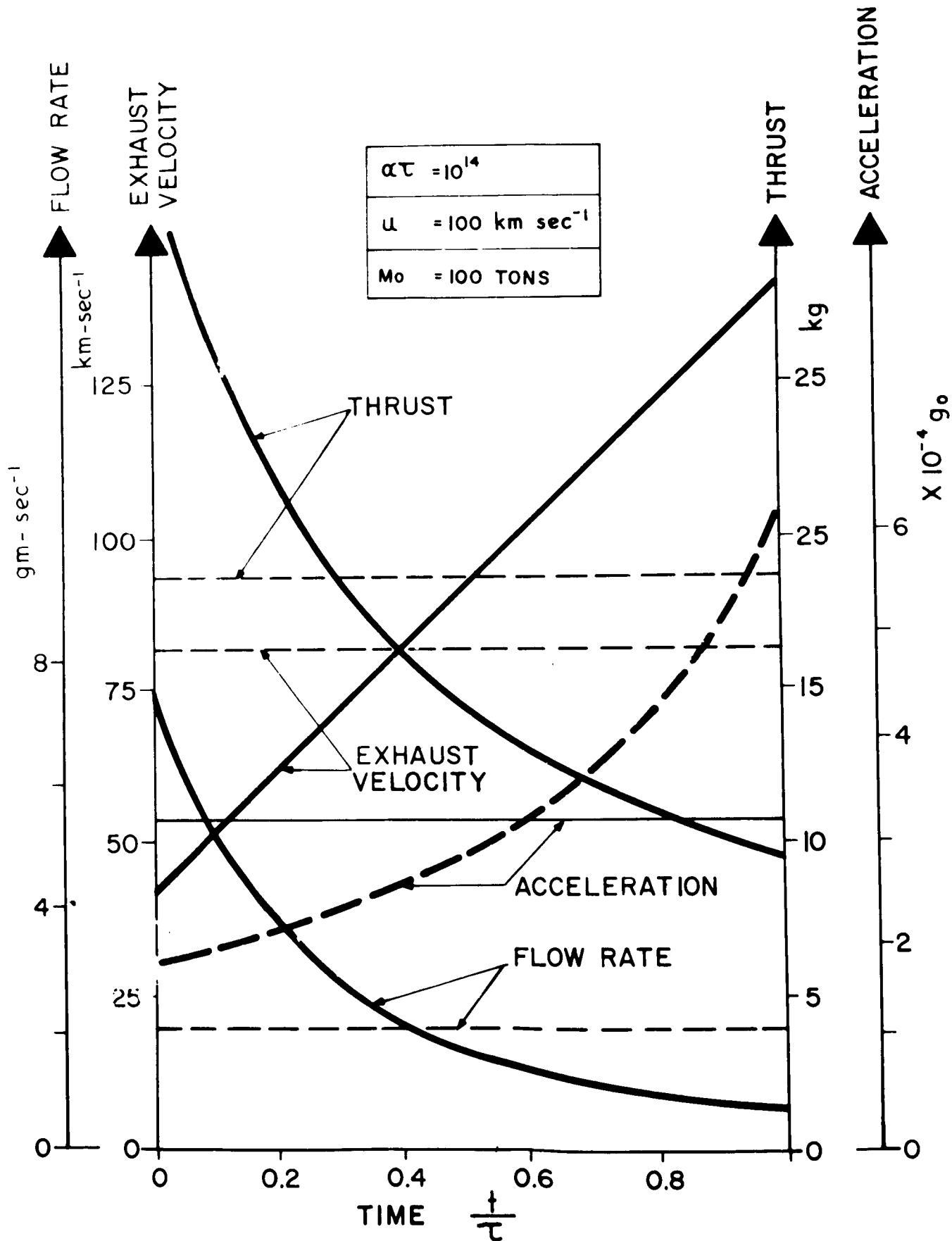


FIG. 8 - Comparison of Propulsion Systems With Constant Thrust (---) and Constant Acceleration (—)

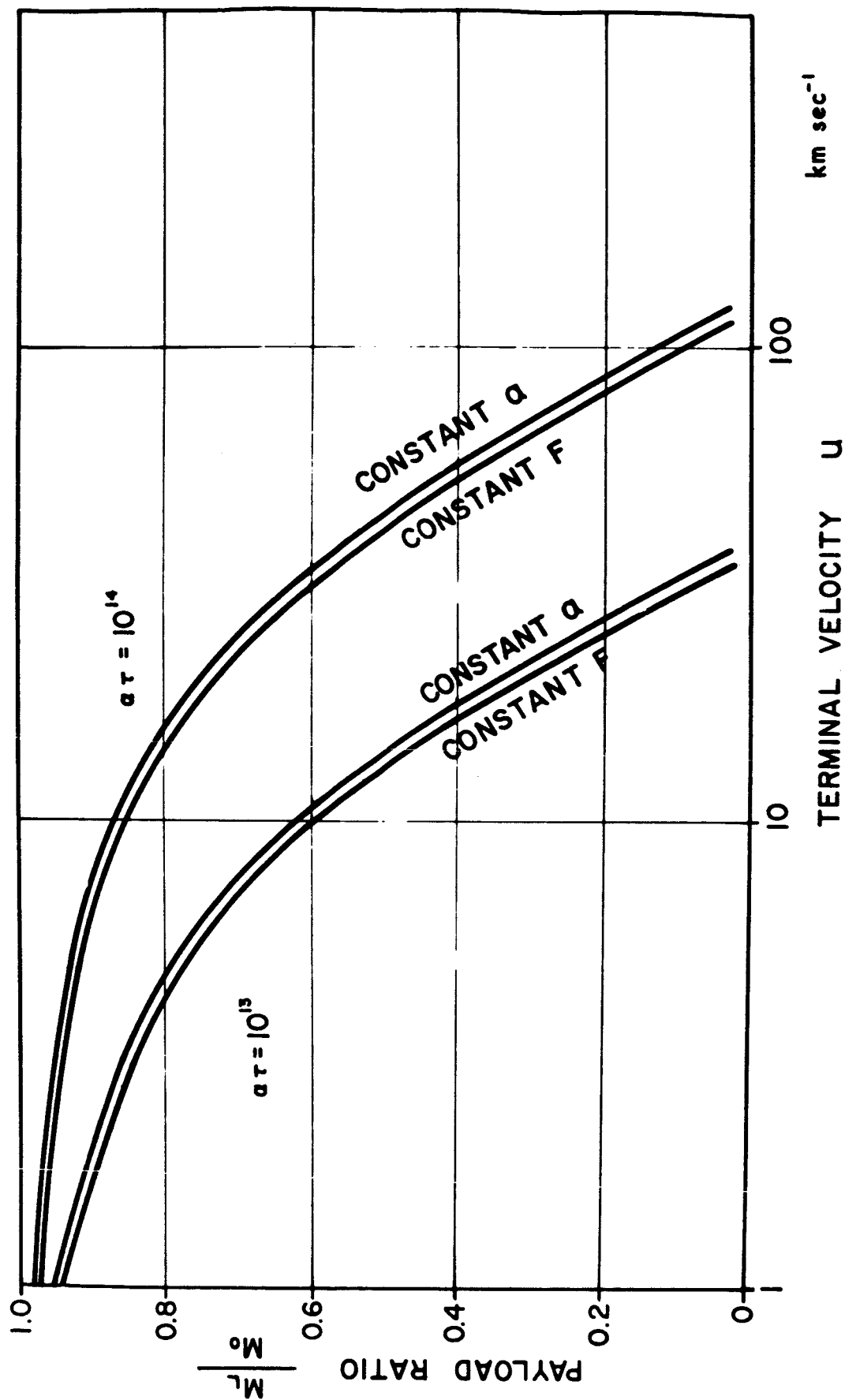
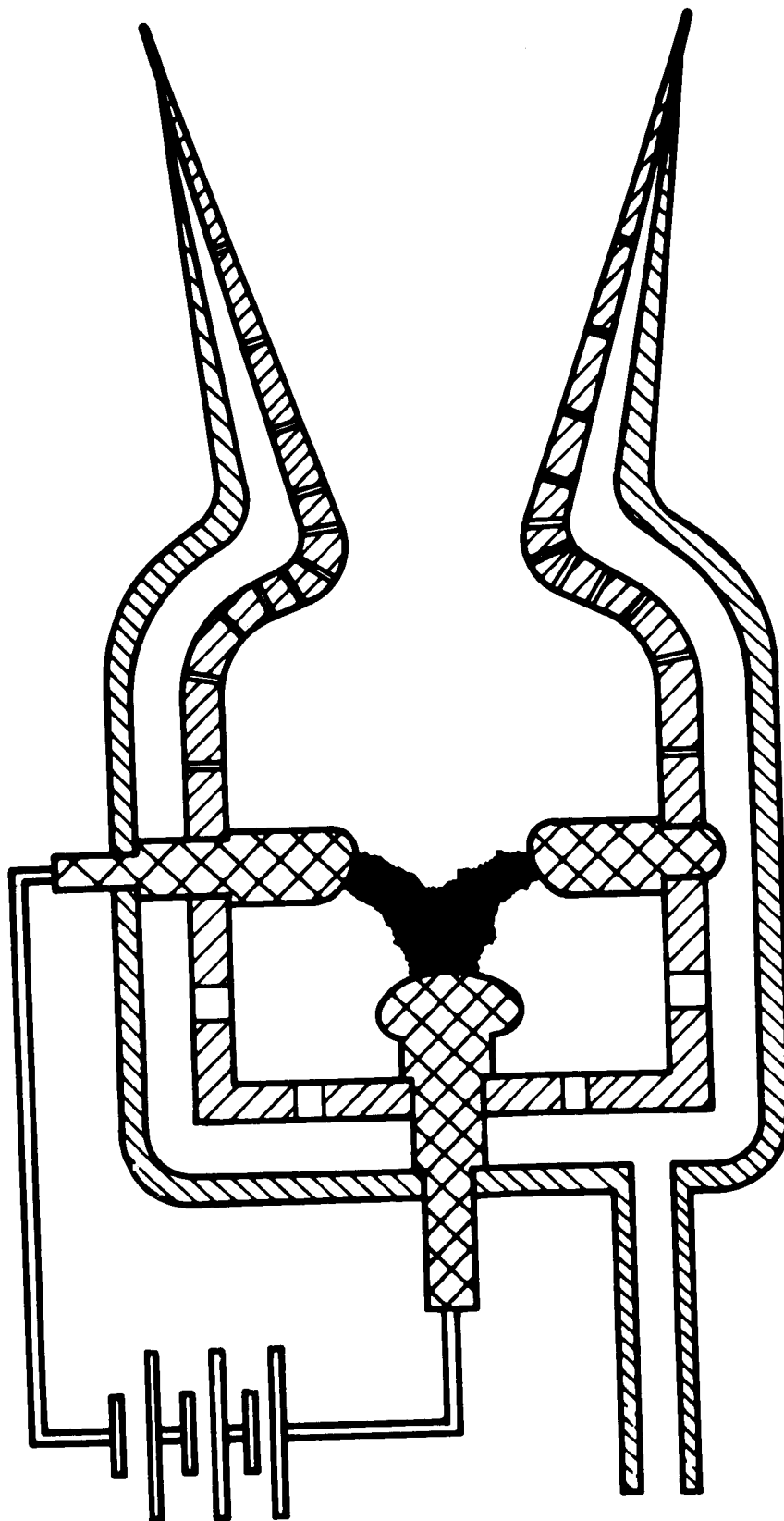


FIG. 9 - Comparison of Propulsion Systems With Constant Acceleration and Constant Thrust



ARC CHAMBER

FIG. 10 - Arc-heated Propulsion Engine

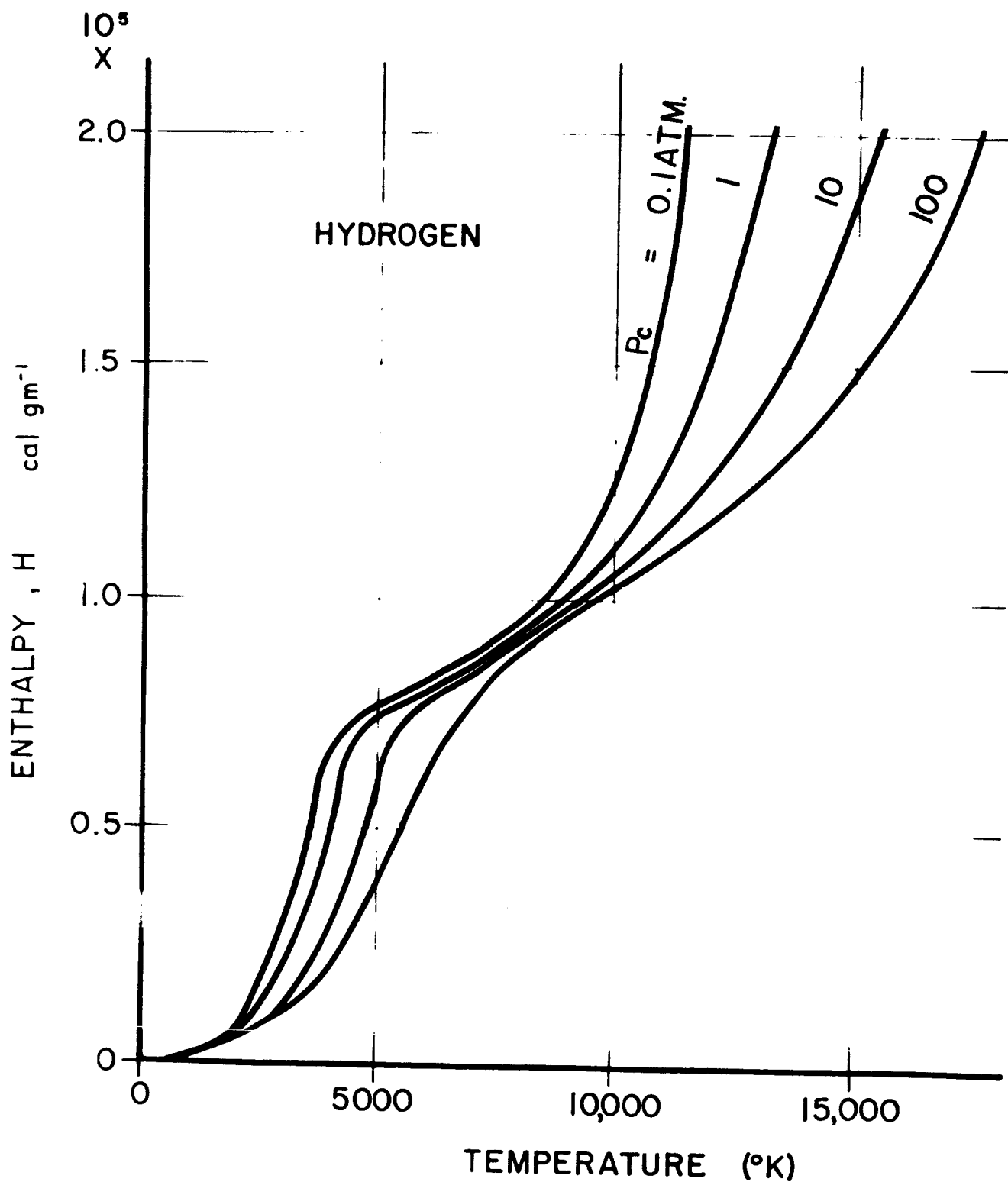


FIG. 11 - Enthalpy of Hydrogen as a Function of Temperature and Chamber Pressure

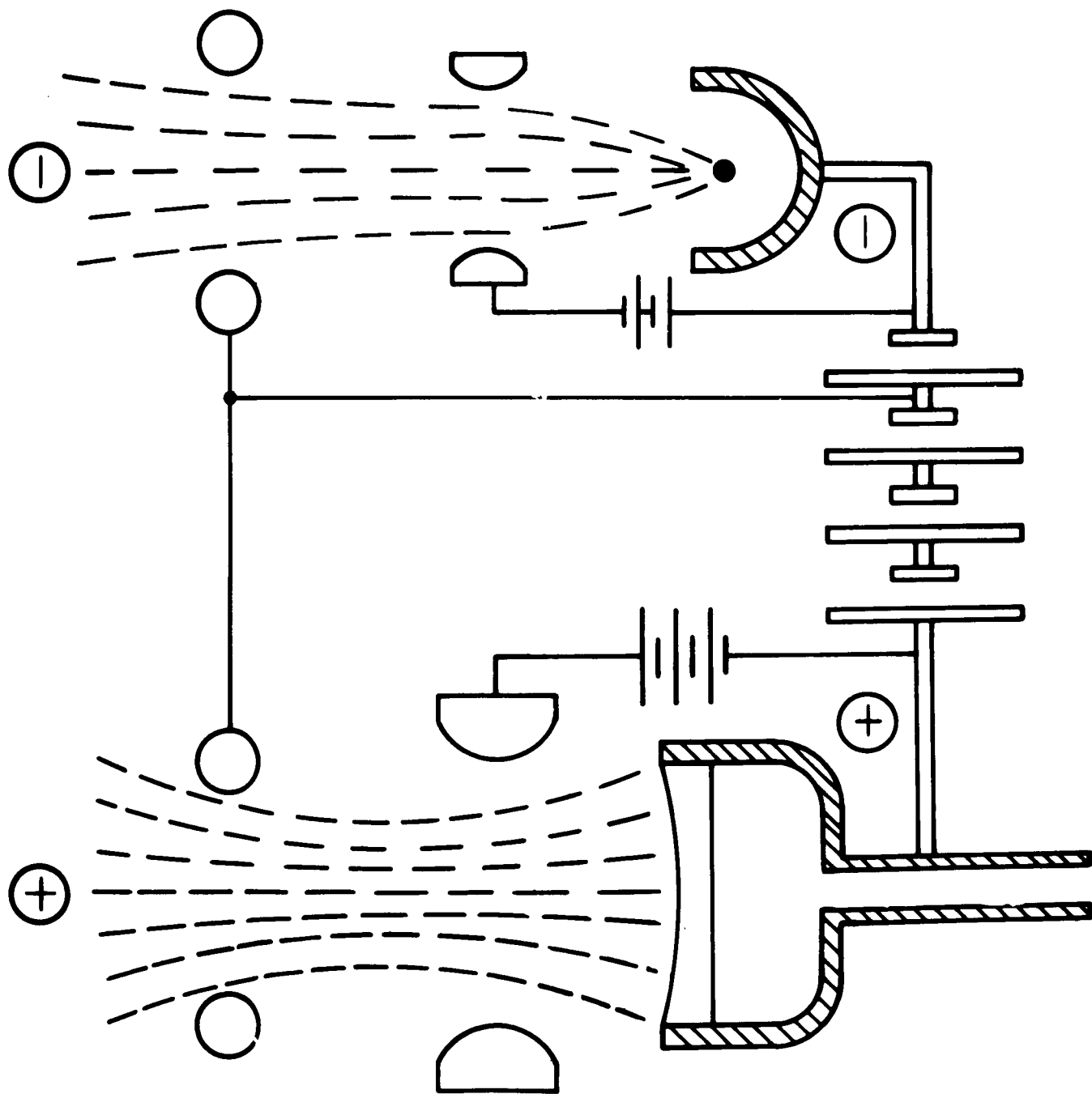


FIG. 12 - Schematic of Ion Propulsion System

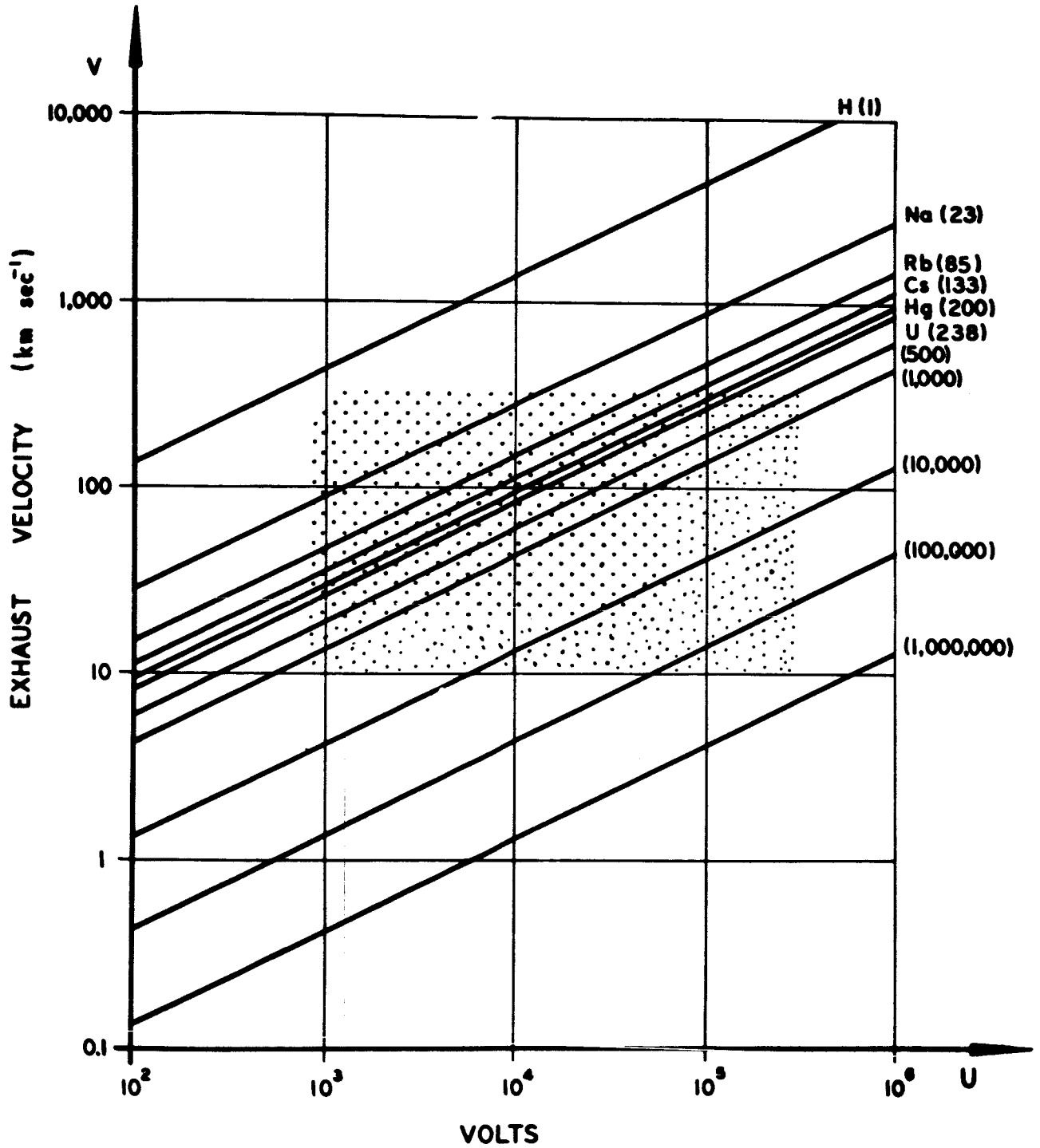
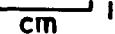


FIG. 13 - Exhaust Velocity as a Function of Particle Mass and Accelerating Voltage (Each particle is assumed to carry one unit charge.)

$$S = 10000 \text{ V cm}^{-1}$$

$$f = 0.08 \text{ g}^* \text{ cm}^{-2}$$

SCALE: 0  1 cm

AREA
ASPECT RATIO
FIELD STRENGTH
POWER
THRUST
EX. VELOCITY
THRUST
THRUST / cm ²
FLOW RATE
$\frac{U_1}{U_2} = \frac{\mu_1}{\mu_2}$
$\frac{I_1}{I_2} = \frac{\mu_2}{\mu_1}$

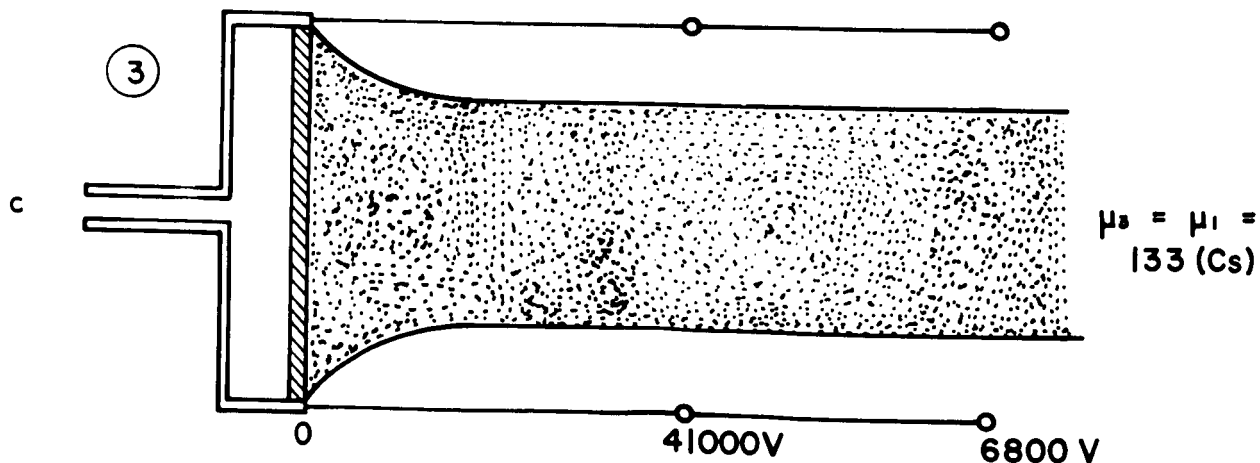
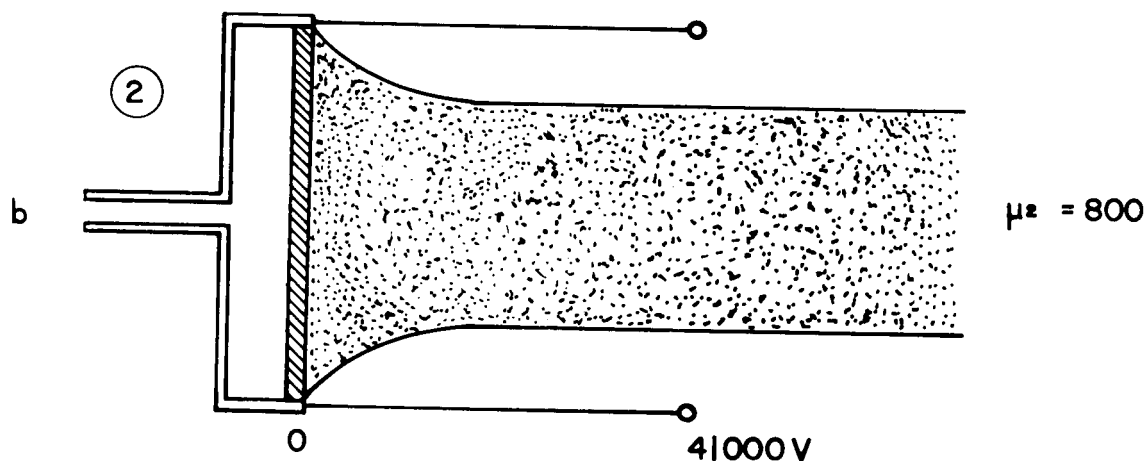
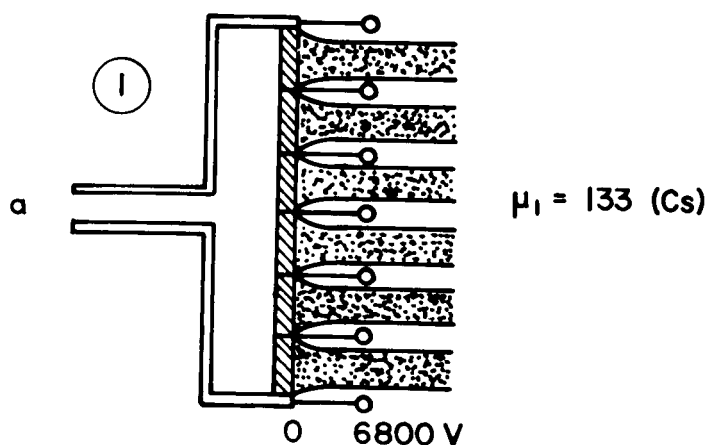


FIG. 14 - Ion Thrust Chambers of Equal Performance (Schematic)

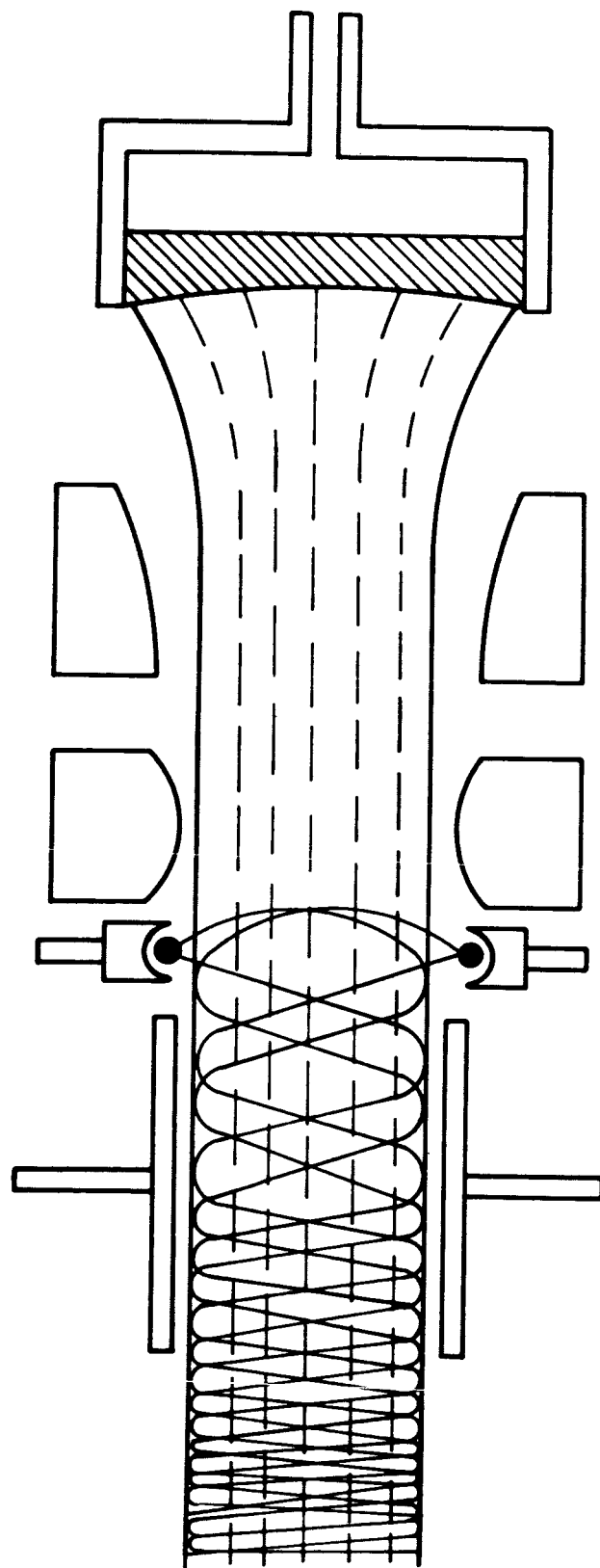


FIG. 15 - Ion Beam With Electron Injection (Schematic)

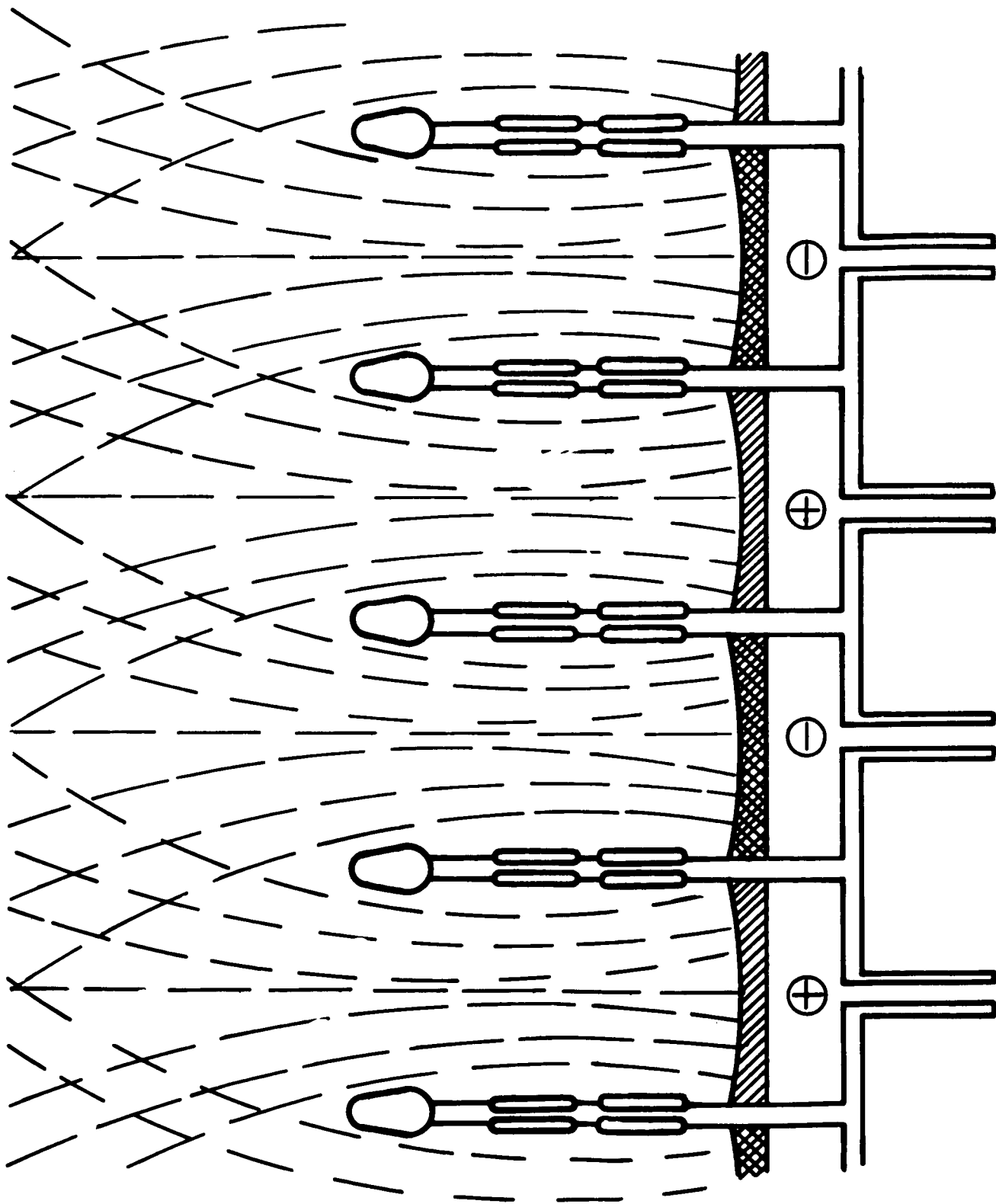


FIG. 16 - Arrangement of Negative and Positive Ion Sources With Acceleration Chambers (Schematic)

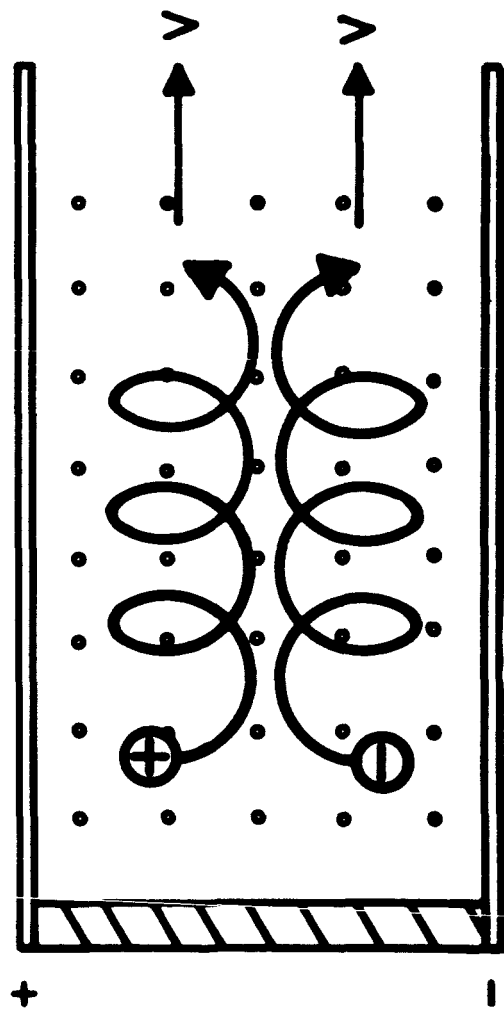
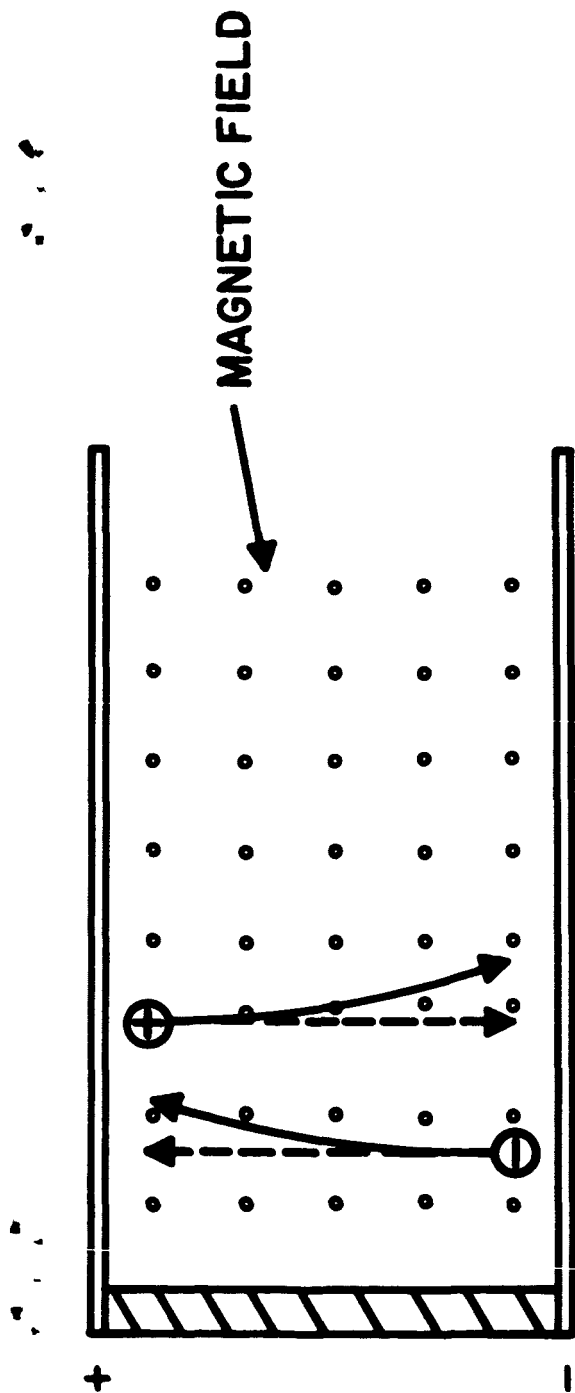


FIG. 17 - Motions of Charged Particles in Electric and Magnetic Fields

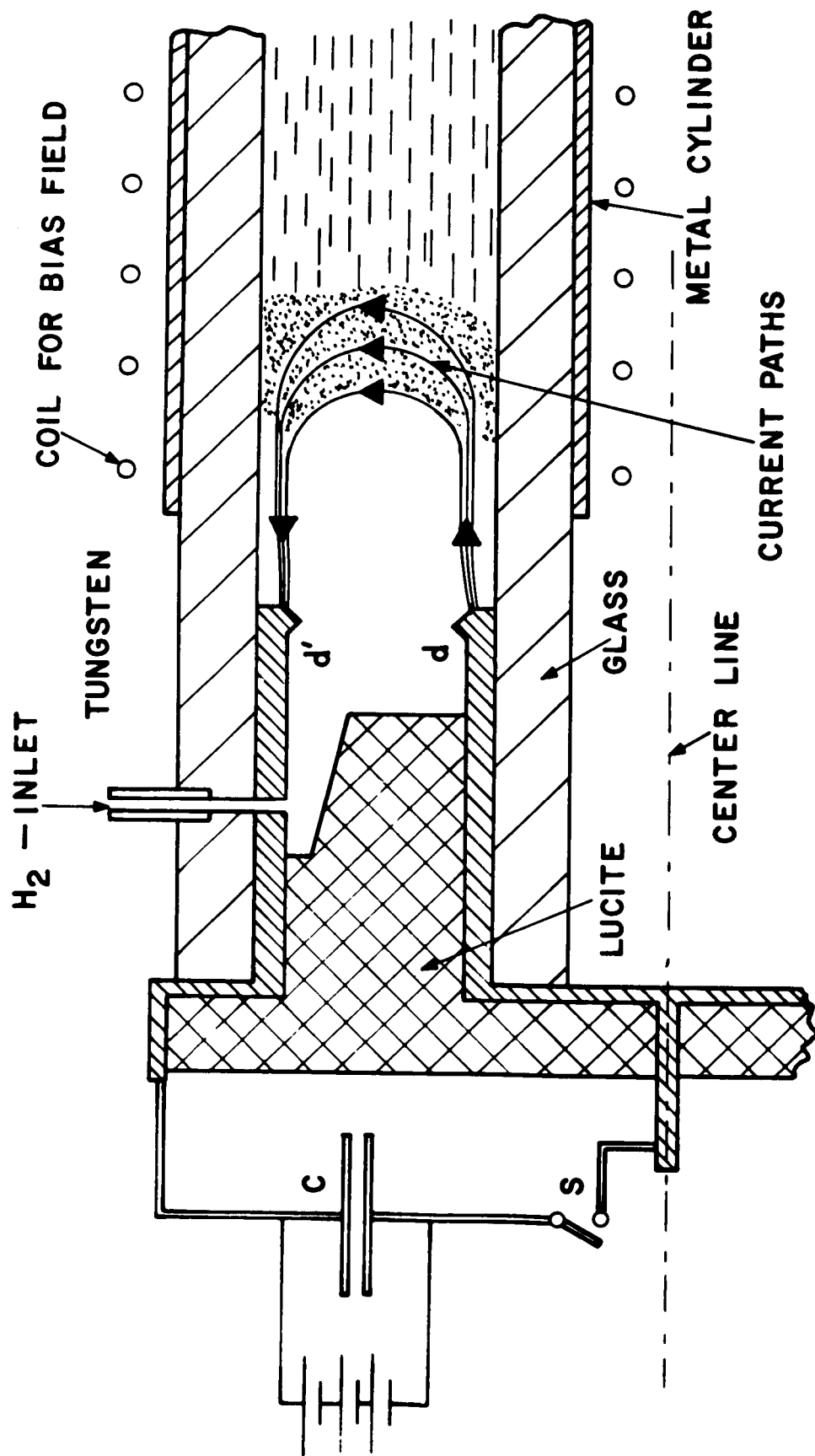


FIG. 18 - Cross Section Through Magnetofluidmechanic Propulsion Engine (Schematic)

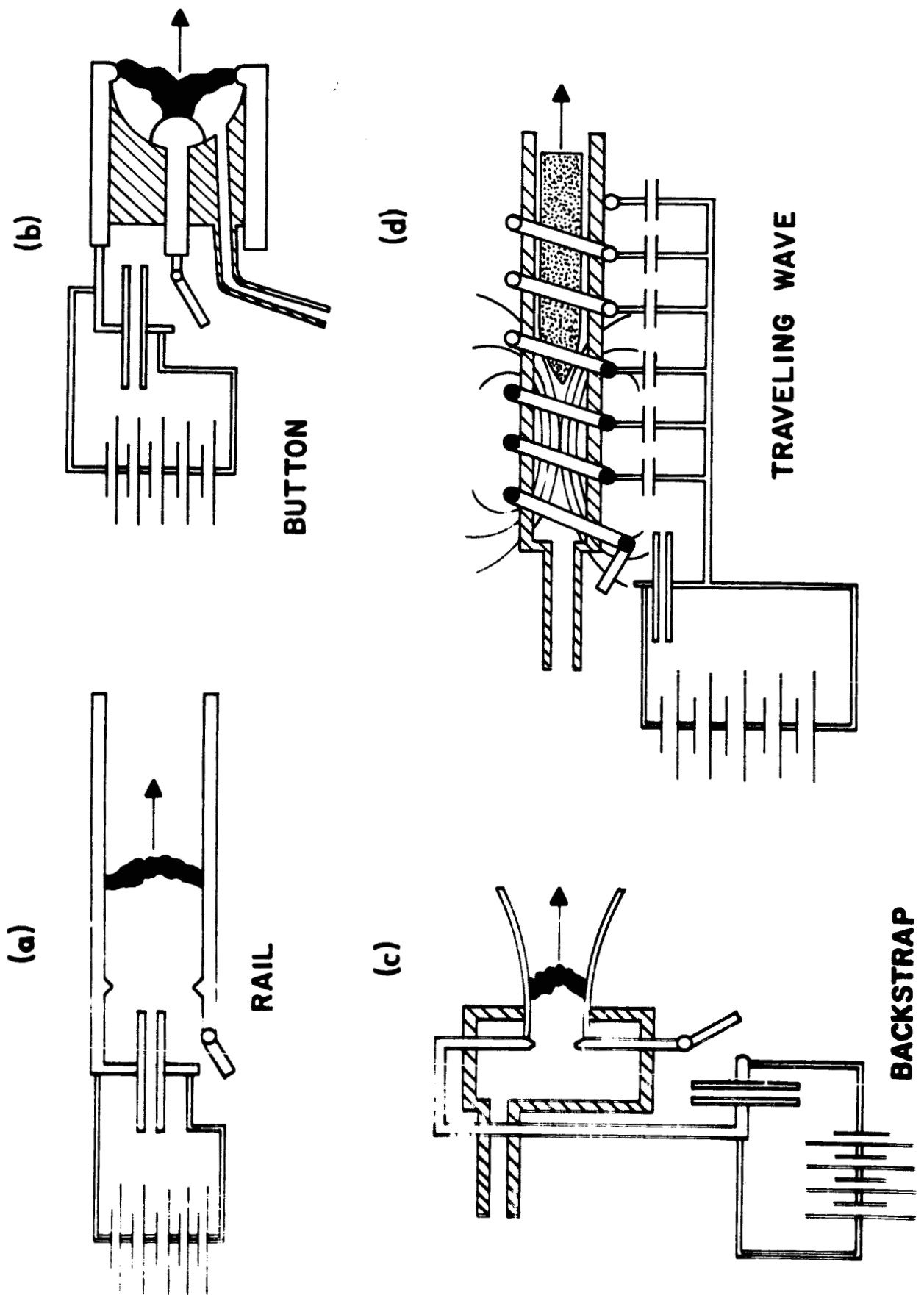


FIG. 19 - Various Types of Electrodynamic Propulsion Systems